TITLE

Population scale mapping of transposable element diversity uncovers novel genetic diversity linked to gene regulation and epigenomic variation

KEYWORDS

Epigenetics, DNA methylation, transposable elements, genomics, Arabidopsis

AUTHORS

Tim Stuart[1], Steven R. Eichten[2], Jonathan Cahn[1], Justin Borevitz[2], Ryan Lister[1]

AFFILIATIONS

1 - ARC Centre of Excellence in Plant Energy Biology, The University of Western Australia, Perth, Australia

2 - ARC Centre of Excellence in Plant Energy Biology, The Australian National University, Canberra, Australia

Corresponding author: Ryan Lister (ryan.lister@uwa.edu.au)

Author ORCID IDs:

0000-0002-3044-0897 (TS)

0000-0003-2268-395X (SRE)

0000-0002-5006-741X (JC)

0000-0001-6637-7239 (RL)

ABSTRACT

Variation in the presence or absence of transposable element (TE) insertions in eukaryotic genomes is a significant source of genetic variation between individuals. Here, we identified 23,095 TE presence/absence variants between 216 wild Arabidopsis accessions. TE variants were identified that were associated with altered expression of nearby genes, indicating a possible functional role in the evolution of gene regulation. A majority of previously identified regions of differential DNA methylation between these accessions were associated with nearby TE variants, indicating an important role in facilitating epigenomic variation. Most TE variants are rare, however more than two thirds of the common alleles identified were not in linkage disequilibrium with nearby SNPs, revealing a potential rich source of missing heritability. An examination of TE regulation following intraspecific crosses between parents with differential TE content revealed that the absence of individual TEs from the paternal genome leads to DNA demethylation within maternal copies of these TEs in the embryo, reminiscent of Drosophila hybrid dysgenesis. This suggests that genetic differences between parents may lead to the formation of DNA methylation differences observed between individuals, and might enable activation of previously silent TEs.

INTRODUCTION

Transposable elements (TEs) are mobile genetic elements present in nearly all studied organisms, and make up a large fraction of most eukaryotic genomes. The two classes of TEs are retrotransposons (class I elements), which transpose via an RNA intermediate requiring a reverse transcription reaction, and DNA transposons (class II elements), which transpose via either a cut-paste or, in the case of Helitrons, a rolling circle mechanism with no RNA intermediate (Wicker et al. 2007). TE activity poses significant mutagenic potential because TE insertion may disrupt essential regions of the genome, and so safeguards have evolved in order to suppress this activity. These safeguards include epigenetic transcriptional silencing mechanisms, chiefly involving the methylation of cytosine nucleotides (DNA methylation) to produce 5-methylcytosine (mC), a mark that can signal transcriptional silencing of the methylated locus. In *Arabidopsis thaliana* (Arabidopsis), DNA methylation occurs in three DNA sequence contexts: mCG, mCHG, and mCHH, where H is any base but G. Establishment of DNA methylation marks can be carried out by two distinct pathways – the RNA-directed DNA methylation pathway guided by 24 nucleotide (nt) small RNAs (smRNAs), and the DDM1/CMT2 pathway (Zemach et al. 2013; Matzke and Mosher 2014). A major function of DNA methylation in Arabidopsis is in the transcriptional silencing of TEs. Loss of DNA methylation due to mutations in genes essential for DNA methylation establishment and maintenance leads to expression of previously silent TEs, and sometimes transposition (Mirouze et al. 2009; Miura et al. 2001; Saze et al. 2003; Lippman et al. 2004; Jeddeloh et al. 1999; Zemach et al. 2013).

TEs are thought to play an important role in evolution, not only because of the disruptive potential of their transposition. The release of transcriptional and posttranscriptional silencing of TEs can lead to bursts of TE activity, quickly generating new genetic diversity on which selection may act (Vitte et al. 2014). TEs may carry regulatory information such as promoters and transcription factor binding sites, and their mobilization may lead to the creation or expansion of gene regulatory networks (Hénaff et al. 2014; Bolger et al. 2014; Ito et al. 2011; Makarevitch et al. 2015). Furthermore, the transposase enzymes required and encoded by TEs have frequently been domesticated and repurposed as endogenous proteins, such as the *DAYSLEEPER* gene in Arabidopsis, derived from a hAT transposase enzyme (Bundock and Hooykaas 2005). Clearly, the activity of TEs can have widespread and unpredictable effects on the host genome. However, the identification of TE presence/absence variants in genomes has remained difficult. It is challenging to identify the structural variants caused by TE mobilization using current short-read sequencing technologies as these reads are typically mapped to a reference genome, which has the effect of masking structural changes that may be present. However, in terms of the number of base pairs affected, a large fraction of genetic differences between Arabidopsis accessions appear to be due to variation in TE content (Cao et al. 2011). Therefore, identification of TE variants is essential in order to develop a more comprehensive understanding of the genetic variation that exists between genomes, and of the consequences of TE movement upon genome and cellular function.

The tools developed previously for identification of novel TE insertion sites have several limitations. They either require a library of active TE sequences, cannot identify TE absence variants, or are not designed with population studies in mind (Thung et al. 2014; Robb et al. 2013; Hénaff et al. 2015). In order to accurately map the locations of TE presence/absence variants with respect to a reference genome, we have developed a novel algorithm, TEPID (Transposable Element Polymorphism IDentification), which is designed for population studies. We tested our algorithm using both simulated and real Arabidopsis sequencing data, finding that TEPID is able to accurately identify TE presence/absence variants with respect to the Col-0 reference genome. We applied our TE analysis method to existing genome resequencing data for 216 different wild Arabidopsis accessions, and identified widespread TE variation amongst these accessions (Schmitz et al. 2013). The majority of these TE variants arose recently in evolutionary times, represent novel genetic variants, and are associated with a variety of epigenomic and transcriptional variation.

RESULTS

Computational identification of TE presence/absence variation

We developed TEPID, an analysis pipeline capable of detecting TE presence/absence variants from paired end DNA sequencing data. TEPID integrates split and discordant read mapping information, read mapping quality, sequencing breakpoints, as well as local variations in sequencing coverage to identify novel TE presence/absence variants with respect to a reference TE annotation (Fig. 1A; see methods). After TE variant discovery has been performed, TEPID then includes a second step designed for population studies. This examines each region of the genome where there was a TE insertion identified in any member of the group, and checks for evidence of this insertion in each member of the population. In this way, TEPID leverages TE variant information for a group of related samples to correct false negative calls within the group. This feature sets TEPID apart from previous similar methods for TE variant discovery using short read data (Hénaff et al. 2015). Testing of TEPID using simulated TE variants in the Arabidopsis genome showed that it was able to reliably detect simulated TE variants (Fig. 1B). In order to assess further the accuracy of TE variant discovery using TEPID, we compared our predicted TE variants identified in the Landsberg *erecta* (L*er*) accession with the *de novo* assembly reference genome created using long sequencing reads. Previously published 100 bp paired-end L*er* genome resequencing reads (Schneeberger et al. 2011) were first analyzed using TEPID, enabling identification of 446 TE insertions and 758 TE absence variants with respect to the Col-0 reference TE annotation (Supplementary File 1). Reads providing evidence for these variants were then mapped to the L*er* reference genome that was generated by *de novo* assembly using Pacific Biosciences P5-C3 chemistry with a 20 kb insert library (Chin et al. 2013), using the same alignment parameters as was used to map reads to the Col-0 reference genome. This resulted in 98.7% of reads being aligned concordantly to the L*er* reference, whereas 100% aligned discordantly or as split reads to the Col-0 reference genome (Table 1). To find whether reads mapped to homologous regions in both the Col-0 and L*er* reference genomes, we conducted a blast search (Camacho et al. 2009) using the DNA sequence between read pair mapping locations in the L*er* genome against the Col-0 genome, and found the top blast result for 80% of reads providing evidence for TE insertions, and 89% of reads providing evidence for TE absence variants in L*er*, to be located within 200 bp of the TE variant reported by TEPID. We conclude that reads providing evidence for TE variants map discordantly or as split reads when mapped to the Col-0 reference genome, but map concordantly to homologous regions of the L*er* *de novo* assembled reference genome, indicating that structural variation is present at the sites identified by TEPID, and that this is resolved in the *de novo* assembled genome.

Abundant TE positional variation among natural Arabidopsis populations

We used TEPID to analyze previously published 100 bp paired-end genome resequencing data for 216 different wild Arabidopsis accessions (Schmitz et al. 2013), and identified 15,007 TE insertions and 8,088 TE absence variants, totaling 23,095 unique TE variants. In most wild accessions we identified 300-500 TE insertions (mean = 378; Fig. S1A) and 1,000-1,500 TE absence variants (mean = 1,279; Fig. S1B), the majority of which were shared by two or more accessions (Fig. S2). PCR validations were performed for a random subset of 10 insertions and 10 absence variants in 14 accessions, and confirmed the high accuracy of TE variant discovery using the TEPID package, with results similar to that observed using simulated data (Fig. 1C, D). TE variants were distributed throughout chromosome 1 in a pattern that is similar to the distribution of all Col-0 TEs, and were enriched in the pericentromeric regions (Fig. 2A, S3). This distribution was also similar to that observed for regions of the genome previously identified as being differentially methylated in all DNA methylation contexts (mCG, mCHG, mCHH) between the wild accessions (population DMRs) (Schmitz et al. 2013). Furthermore, TE variants were depleted within genes and DNase I hypersensitivity sites (Sullivan et al. 2014), while they were enriched in gene flanking regions and within other annotated TEs or pseudogenes (Fig. 2B).

Among the identified TE variants, several TE superfamilies were over- or under-represented compared to the number expected by chance given the overall genomic frequency of different TE types (Fig. 2C; Table S1, S2). In particular, TE variants in the RC/Helitron superfamily were less numerous than expected, with an 11.5% depletion of RC/Helitron elements in the set of TE variants. TEs belonging to the LTR/Gypsy superfamily were more variable than expected, with a 7.5% enrichment in the set of TE variants. This was unlikely to be due to a differing ability of our detection methods to identify TE variants of different lengths, as the TE variants identified had a similar distribution of lengths as all Arabidopsis TEs annotated in the Col-0 reference genome (Fig. S4A-C). These enrichments suggest that the RC/Helitron TEs have been relatively dormant in recent evolutionary history, while the LTR/Gypsy TEs have been more active. At the family level, we observed similar patterns of TE variant enrichment or depletion (Fig. S5). As expected, this TE diversity tended to reflect the known genetic relationships between accessions. We further examined Arabidopsis (Col-0) DNA sequencing data from a transgenerational stress experiment to investigate the possible minimum number of generations required for TE variants to arise (Jiang et al. 2014). We identified a single potential TE insertion in a sample following 10 generations of single-seed descent under high salinity stress conditions, and no TE variants in the control single-seed descent set. However, without experimental validation it remains unclear if this represents a true variant. Therefore, we conclude that TE variants likely arise at a rate less than 1 insertion in 30 generations.

Although thousands of TE variants were identified, it is important to classify their relationship to other commonly identified sources of genetic variation such as single nucleotide polymorphisms (SNPs). This comparison can determine if TE variants are often in linkage disequilibrium with nearby SNPs, or if they are a previously unassessed source of genetic variation between accessions unlinked to the underlying SNP-based haplotypes. To investigate this relationship, SNPs previously identified between the wild accessions (Schmitz et al. 2013) were compared to the presence/absence of individual TE variants. For the 7,300 testable TE variants in the sample set with a minor allele frequency above 3%, the nearest 300 flanking

SNPs upstream and downstream of the TE insertion site were analyzed for linkage disequilibrium (LD, r^2; Fig. 2D-F; see methods). TE variants were classified as being either ‘young’, ‘mid’, or ‘old’ variants by comparing ranked r^2 values to flanking SNPs against the median ranked r^2 value for all SNP-SNP comparisons to account for regional variation in LD (Fig. 2D, E). This analysis identified TE variants that were unlinked (young) or linked (old) to SNPs forming local haplotypes, or were in an intermediate linkage state (mid) with their surrounding haplotype. The majority (61%) of testable TE variants were largely unlinked to nearby SNPs, and are therefore predicted to be young variants present in a few divergent accessions (Fig. 2F). In contrast, 29% of TE variants displayed high levels of linkage with nearby SNPs, and are likely old insertions. TE variants displayed a similar chromosomal distribution regardless of age classification (Fig. 2G). Overall, this analysis revealed an abundance of previously unexplored genetic variation that exists amongst Arabidopsis accessions caused by the presence or absence of TEs, and illustrates the importance of identifying TE variants to capture missing heritability alongside other genetic diversity such as SNPs.

TE variants affect gene expression

To determine whether the TE variants identified affected nearby gene expression, we compared the steady state transcript abundance within mature leaf tissue, between accessions with and without TE insertions, for genes with TE variants located in the 2 kb gene upstream region, 5’ UTR, exon, intron, 3’ UTR or 2 kb downstream region (Fig. 3). While the steady state transcript abundance of most genes appeared to be unaffected by the presence of a TE, 45 genes displayed significant differences in transcript abundance linked with the presence of a TE variant, indicating a functional role for these variants in the local regulation of gene expression (q-value < 0.001 with greater than 2-fold change in transcript abundance; Fig. 3, Table 2). We did not find any functional category enrichments in this set of differentially expressed genes. It should be noted that rare TE variants, with a minor allele frequency less than 3%, may also be associated with a difference in transcript abundance, but were unable to be statistically tested due to their rarity. Future studies using larger sample sizes may be able to further examine the frequency at which TE variants impact gene expression.

As both increases and decreases in transcript abundance of nearby genes were observed for TE variants within each gene feature, it appears to be difficult to predict the impact a TE variant may have on nearby gene expression. However, gene-level transcript abundance measurements may fail to identify the potential positional effect of TE variants upon transcription. To more closely examine changes in transcript abundance associated with TE variants among the accessions, we inspected a subset of TE variant sites and identified TE variants that appear to have an impact on transcriptional patterns beyond changes in total transcript abundance. For example, the presence of a TE within an exon of *AtRLP18* (AT2G15040) was associated with truncation of the transcripts at the TE insertion site in accessions possessing the TE variant, as well as silencing of a downstream gene encoding a leucine-rich repeat protein (AT2G15042) (Fig. 4A-D). Both genes have significantly lower transcript abundance in accessions containing the TE insertion ($p < 5.8 \times 10^{-10}$, Mann-Whitney U test; Fig. 4C). *AtRLP18* is reported to be involved in bacterial resistance, with the disruption of this gene by T-DNA insertion mediated mutagenesis resulting in increased susceptibility to the bacterial plant pathogen *Pseudomonas syringae* (Wang et al. 2008). We examined pathogen resistance phenotype data (Aranzana et al. 2005) for accessions with and without a TE insertion in the *AtRLP18* exon, and found that accessions containing the TE insertion were sensitive to infection by *Pseudomonas syringae* transformed with *avrPpH3* genes at a much higher frequency (Fig. 4E). This suggests that the wild accessions identified here to contain a TE insertion within *AtRLP18* may have an increased susceptibility to certain bacterial pathogens.

We also observed some TE variants associated with increased expression of nearby genes. For example, presence of a TE within the upstream region of a gene encoding a pentatricopeptide repeat (PPR) protein (AT2G01360) was associated with higher steady state transcript abundance of this gene (Fig. 4F-H). Interestingly, transcription appeared to begin at the TE insertion point, rather than the transcriptional start site of the gene (Fig. 4F). Accessions containing the TE insertion had significantly higher AT2G01360 transcript abundance than the accessions without the TE insertion ($p < 1.8 \times 10^{-7}$, Mann-Whitney U test; Fig. 4H). The apparent transcriptional activation, linked with presence of a TE belonging to the *HELITRON1* family, indicates that this element may carry sequences or other regulatory information that has altered the expression of genes downstream of the TE insertion site. Importantly, this variant was classified as a young TE insertion, as it is not in linkage disequilibrium with surrounding SNPs, and therefore the associated changes in gene transcript abundance would not be identified using only SNP data. This TE variant was also upstream of *QPT* (AT2G01350), involved in NAD biosynthesis (Katoh et al. 2006), which did not show alterations in steady state transcript abundance associated with the presence of the TE variant, indicating a potential directionality of regulatory elements carried by the TE (Fig. 4G, H). Overall, these examples demonstrate that TE variants can have unpredictable, yet important, effects of the expression of nearby genes, and these effects may be missed by studies focused on genetic variation at the level of SNPs.

TE variants drive DNA methylation differences between accessions

As TEs are frequently highly methylated in Arabidopsis (Lister et al. 2008; Cokus et al. 2008; Zhang et al. 2006; Zilberman et al. 2007), we next assessed the DNA methylation state surrounding TE variant sites to determine whether TE variants might be responsible for some of the differences in DNA methylation patterns previously observed between the wild accessions

(Schmitz et al. 2013). We found that 61% of the 13,485 previously reported population DMRs were located within 1 kb of a TE variant, significantly more than expected by chance ($p < 1 \times 10^{-4}$, determined by resampling 10,000 times; Fig. 5A). Old TE variants were more often located close to population DMRs, with 41.5% of TE variants within 1 kb of a population DMR classified as old, 11.5% higher than the total genomic frequency of old elements (Fig. 5B). There was a corresponding depletion of young TE variants in this set, with 48.5% being classified as young, 11.5% lower than the total genomic frequency of young TE variants. This indicates that established TE insertions may be more important than recent TE insertions in defining DNA methylation landscapes. Alternatively, unmethylated TEs may be preferentially lost from the population due to selection, resulting in old TE variants being more highly methylated. DNA methylation levels at population DMRs located within 1 kb a TE variant, henceforth termed TE-DMRs, were positively correlated with the presence of the TE variant (Fig. 5C), while DNA methylation levels at population DMRs further than 1 kb from a TE variant did not have a significant association with the presence/absence of the nearest TE variant. TE-DMRs were significantly more highly methylated in accessions containing the TE, suggesting that TE variants may facilitate changes in DNA methylation patterns between accessions (Welch's t-test, $p < 2.2 \times 10^{-16}$; Fig. 5D). Overall, this indicates that a large fraction of the population DMRs previously identified between these accessions are associated with the presence of local TE insertions.

We next examined levels of DNA methylation in regions flanking all TE insertions regardless of the presence or absence of a population DMR call, and similarly found that accessions containing a TE insertion had a highly localized enrichment in DNA methylation in all sequence contexts (Fig. 5E, F), again indicating that TE variants may play a role in shaping DNA methylation landscapes between Arabidopsis accessions. As the increase in DNA methylation around TE insertion sites appeared to be restricted to regions >200 bp from the insertion site, we correlated DNA methylation levels in 200 bp regions flanking TE variants with the presence/absence of TE variants. DNA methylation levels were positively correlated with the presence of a TE (Fig. 5G). Furthermore, DNA methylation level was more strongly correlated with the presence of old TE variants. These results indicate that DNA methylation patterns are influenced by the differential TE content of individual genomes, and that the DNA methylation-dependent silencing of TE variants may lead to formation of DMRs between wild Arabidopsis accessions. The age of TE variants also appears to be related to the DNA methylation state surrounding the TE insertion site, with older variants being more highly methylated, suggesting that many generations may be required before a new TE insertion reaches a highly methylated state.

TE regulation in the germline

To explore when during development germline changes in TE content may occur, we sought to associate TE DNA methylation dynamics during germline development and early embryogenesis with the differential TE content we observe between the different Arabidopsis accessions. Complex DNA methylation changes occur in the Arabidopsis germline, particularly within TE sequences. During male germline development, the haploid microspore undergoes asymmetric division to produce the larger vegetative cell and a smaller cell that divides once more to produce two identical sperm cells (Fig. 6A) (Kawashima and Berger 2014). Some TEs have previously been found to become transcriptionally active and to transpose in the vegetative cell nucleus (VN). This TE activation has been linked to an increase in 21 nt smRNAs derived from activated TE sequences, that are thought to then be transported to the sperm cells (Slotkin et al. 2009). In contrast, the sperm and post-meiotic microspore genomes lose DNA methylation in the mCHH context within many TEs due to decreased DRM2 abundance but are able to maintain TE silencing (Slotkin et al. 2009; Calarco et al. 2012). A largely distinct set of

TEs are demethylated in the mCG context in the VN compared to the microspore and sperm cells, and are thought to be involved in epigenetic imprinting rather than TE silencing (Calarco et al. 2012). In the female germline, the ovule contains a diploid central cell and haploid egg cell. As in the VN, the non-generative central cell acts as a companion to the egg and expresses *DEMETER*, which encodes a DNA demethylase, resulting in global DNA demethylation (Ibarra et al. 2012). During fertilization, one sperm fertilizes the egg to form the diploid embryo, while the other sperm fertilizes the diploid central cell to form the triploid endosperm, which supplies nutrients to the developing embryo (Fig. 6A) (Kawashima and Berger 2014). The endosperm remains globally demethylated, while DNA methylation is gradually restored in the embryo through RdDM (Jullien et al. 2012; Hsieh et al. 2009).

In order to determine whether these TEs that undergo DNA methylation changes in the male germline or in the embryo and endosperm are especially active elements, we examined both the number of unique insertions caused by these differentially methylated elements (transposition frequency), as well as the presence/absence variability of these TEs among the wild accessions (Fig. 6B, C) (Hsieh et al. 2009; Calarco et al. 2012). We found that 68% of TEs previously found to be demethylated in the mCHH context in Col-0 sperm and microspore were absent from non-Col-0 accessions (Fig. 6B), a much larger fraction than expected by chance ($p < 1 \times 10^{-4}$, determined by resampling 10,000 times) (Calarco et al. 2012). In contrast, TEs differentially methylated in the mCG context in the sperm or microspore, thought to be involved in epigenetic imprinting, or in the mCHH context in the developing embryo (Hsieh et al. 2009), were not absent from non-Col-0 accessions significantly more often than expected ($p > 0.09$, determined by resampling 10,000 times; Fig. 6B). While TEs mCG-hypomethylated in the endosperm were absent from non-Col-0 genomes significantly more often than expected ($p < 1 \times 10^{-4}$, determined by resampling 10,000 times), the scale of this difference was small, with only 30% of the TEs absent in non-Col-0 accessions. mCHH-demethylated TEs in the sperm and microspore also had a significantly higher transposition frequency, suggesting that they have been more active than most other TEs in the Arabidopsis genome (Fig. 6C; Welch's t-test, $p < 1 \times 10^{-5}$). While mCHH-hypermethylated TEs in the embryo were not found to be frequently absent from non-Col-0 accessions, these elements did show a significantly higher transposition frequency, as did elements mCG-hypomethylated in the endosperm, indicating that demethylation of active TEs in the germline companion cells (the VN and endosperm) may be important in driving DNA methylation changes in the generative cells (the sperm and embryo), perhaps acting to suppress transposition of active elements in the germline.

TEs that are demethylated in the mCHH context in the developing sperm may rely on smRNAs in the seed for the restoration of proper DNA methylation of paternal TE sequences in the embryo following fertilization, through RdDM (Jullien et al. 2012). These smRNAs are thought to be maternally-derived, and are likely produced in the endosperm (Mosher et al. 2009; Calarco et al. 2012). We sought to determine whether TEs present in only one parental genome in an intraspecific cross would show altered levels of smRNAs targeted to these TEs, as the absence of a TE in the maternal genome may lead to the loss of a maternally-derived smRNA signal in the seed. Using previously published whole seed 21-24 nt smRNA data for reciprocal crosses between Col-0 and Cvi or L*er* (Pignatta et al. 2014; Gehring et al. 2014), we examined seed smRNA levels in TEs present in the Col-0 genome but absent from the Cvi genome for crosses between Col-0 and Cvi, or absent from the L*er* genome for crosses between Col-0 and L*er* (Fig. 6D, direction of each cross is depicted as *female x male* on axis labels). Consistent with previous reports, we found that smRNA levels in TEs were dependent on maternal genotype but independent of paternal genotype, indicating that they are maternally-derived. Furthermore, we confirmed that TEs present in only the paternal genome in a cross had significantly lower 21-24 nt smRNA levels compared with crosses where the TE was present in the maternal genome ($p < 1.4 \times 10^{-10}$, Mann-Whitney U test; Fig. 6E). As these smRNAs are thought to be required for TE silencing in the embryo (Jullien et al. 2012; Matzke and Mosher 2014), this may then lead to TE activation and may explain the higher transposition frequencies we observe for TEs demethylated in the mCHH context in the sperm genome.

To test whether the absence of a TE in the maternal genome was sufficient to prevent the re-methylation of the paternal copy of that TE following fertilization, we examined previously published embryonic DNA methylation data within Cvi-absent TEs following reciprocal crosses between Col-0 and Cvi (Pignatta et al. 2014) (Fig. 6F). For all crosses between Col-0 and Cvi, Cvi-absent TEs showed significantly lower mCG levels, and this is likely due to the global reduction in mCG levels that exists in the Cvi genome rather than the absence of the TE in one parent (Pignatta et al. 2014). Surprisingly, we found for TEs that lose mCHH in the sperm (Calarco et al. 2012), when the TE was absent from the maternal genome (Cvi x Col-0), embryonic mCHH levels within these TEs were not significantly different from DNA methylation levels in the Col-0 x Col-0 cross, where the TE was present in both parents ($p > 0.04$, Mann-Whitney U test; Fig. 6F). This was contrary to the anticipated pattern, where the loss of maternal smRNAs observed for this cross (Fig. 6E) would prevent these sperm-demethylated TEs from being re-methylated in the embryo, and may indicate that maternally-derived smRNAs are not essential for establishing DNA methylation patterns in early embryonic development. However, when the parents were reversed and the TE variants were present in the maternal genome but absent from the paternal genome (Col-0 x Cvi), we found a significant reduction in mCHH methylation for these TEs, indicating that paternal signals may be required for DNA methylation of maternal TE sequences ($p < 5 \times 10^{-7}$, Mann-Whitney U test). To further investigate this result, we analyzed an independent dataset containing embryonic DNA methylation data for crosses between Col-0 and L*er*, generated at a slightly later developmental stage (7-8 days after pollination) than the data for crosses between Col-0 and Cvi (6 days after pollination). Within TEs absent from L*er* and demethylated in the Col-0 sperm (Ibarra et al. 2012) we found no significant difference in DNA methylation levels in any context dependent on the parental genotypes (Fig. S6). This could indicate that embryonic DNA methylation changes within maternal TEs, dependent upon paternal genotype, may be restricted to early developmental time points, less than 6 days after pollination, or may be dependent on the intraspecific cross performed.

Considering the high proportion of sperm mCHH-demethylated TEs that were found to be absent in non-Col-0 accessions (Fig. 6B), crosses between plants with differential presence/absence of these TEs may be possible in the wild, and such crosses may lead to the demethylation of the maternal copies of these TEs in the embryo when a paternal copy is absent. These findings support a model for TE silencing escape facilitated by genetic differences between parents, as the loss of DNA methylation within TEs has been shown previously to be sufficient for transcriptional activation and transposition of demethylated TEs (Gendrel et al. 2002; Hirochika et al. 2000; Stroud et al. 2013). Such mating situations may also lead to the formation of stable epialleles depending of the length of time the TE sequences are able to escape remethylation, and this may play a role in formation of the patterns of differential DNA methylation previously observed between wild accessions (Schmitz et al. 2013).

DISCUSSION

Here, we discovered widespread differential TE content between wild Arabidopsis accessions. A subset (32%) of TE variants with a minor allele frequency above 3% were able to be tested for linkage with nearby SNPs. The majority of these TE variants were unlinked to surrounding SNPs, indicating that they represent genetic variants currently overlooked in genomic studies. We found a marked depletion of TE variants within gene bodies and DNase I hypersensitivity sites, indicating that the more deleterious TE insertions have likely been removed from this population through selection. Importantly, we were able to identify examples where TE variants appear to have an effect upon gene expression, both in the disruption of transcription and in the spreading or disruption of regulatory information leading to the transcriptional activation of genes, indicating that these TE variants can have important consequences upon expression of protein coding genes. Furthermore, we provide evidence that differential TE content between genomes of wild Arabidopsis accessions underlies a large fraction of the previously reported DNA methylation differences between accessions. Thus, the frequency of pure epialleles, independent of underlying genetic variation, may be even more rare than previously anticipated (Richards 2006). The level of DNA methylation changes associated with TE variants is related to TE age, with old variants being more strongly correlated with increased DNA methylation levels. This suggests that the methylation of new TE insertions is a gradual process that occurs incrementally over many generations, or that unmethylated TEs are preferentially lost from the population over time.

Identification of TE variants between Arabidopsis accessions has also enabled a closer examination of the changes in TE smRNA and DNA methylation levels following fertilization of intraspecific hybrids. smRNA levels in the seed appear to be dependent on maternal genome content, as the presence of a TE in only the paternal genome of a cross is associated with decreased levels of corresponding 21-24 nt smRNAs derived from those TEs in the seed. This loss of smRNAs, dependent on maternal genotype, is strikingly similar to findings from studies performed in *Drosophila melanogaster* over 3 decades ago, where maternal absence of paternal *P* elements in a cross was found to lead to activation and frequent transposition of these *P* elements, due to absence of maternally-derived smRNA signals needed for TE silencing, while TE activation was not observed when the *P* elements were present in the maternal genome (Bingham et al. 1982; Blumenstiel and Hartl 2005). This is thought to be the underlying cause of hybrid dysgenesis, a phenotype characterized by sterility and high rates of germline TE activity, and where the transpositions caused by active *P* elements are often lethal to the hybrid offspring. It has been hypothesized previously that a process similar to Drosophila hybrid dysgenesis may occur in Arabidopsis, as smRNAs in the Arabidopsis seed also appear to be maternally-derived, and there is some prior evidence that this may be true (Martienssen 2010). Interspecific crosses between *Arabidopsis thaliana* females and *Arabidopsis arenosa* males was observed to lead to the expression of previously silent paternal *ATHILA* TEs, thought to be due to the presence of *ATHILA* elements in the *A. arenosa* genome that are absent from the *A. thaliana* genome (Josefsson et al. 2006). However, the reciprocal cross is impossible to generate due to pollination failure, constituting a fundamental limitation of this system for studying hybrid dysgenesis. The use of wild *A. thaliana* accessions may prove more fruitful in future experiments aiming to elucidate the processes of germline TE regulation in plants.

Surprisingly, we found that this decrease in smRNA levels targeting paternal TE sequences was not linked to DNA demethylation of the corresponding paternal TEs in the embryo, but instead observed an inverse relationship, where TEs absent from the paternal genome in a cross were linked with embryonic demethylation of the maternal copy. This indicates that maternal smRNAs are not essential for restoring the paternal patterns of DNA methylation that are erased in the sperm, nor are they sufficient to maintain DNA methylation within maternal TEs in the absence of paternal TE copies. As 21 nt smRNA production is greatly increased within the pollen VN, and these smRNAs may be transported to the sperm cells (Slotkin et al. 2009), it is possible that these paternal smRNAs remain present in the sperm cytoplasm during fertilization. These smRNAs may play an important role in establishing early patterns of DNA methylation in the embryo, perhaps explaining the non-reliance of paternal TE sequences upon maternal smRNAs. This issue is somewhat complicated by the lack of embryo-specific smRNA data, as all existing data have been generated from whole seed. If maternal smRNAs are produced and remain in the endosperm rather than the embryo, this could further explain the apparent reliance upon paternal silencing signals for proper establishment of DNA methylation patterns following fertilization. Our data provides the first evidence that embryonic TE silencing in Arabidopsis may be dependent on paternal, rather than maternal, silencing factors.

DNA methylation changes triggered by genetic differences between parents clearly occur in Arabidopsis, although perhaps via a different mechanism as is responsible for causing hybrid dysgenesis in Drosophila. These DNA methylation changes that occur in the embryo may play an important role in the formation of DNA methylation differences between wild Arabidopsis accessions, depending on the length of time these changes are able to persist in hybrid progeny. If the loss of DNA methylation within maternal TEs that we observe is able to persist in hybrid plants, this may lead to the formation of stable epialleles as the demethylated TE copy is propagated through the population. Further experiments will be required to determine the stability of these embryonic changes in DNA methylation that occur in hybrid plants. Alternatively, if these DNA methylation changes are limited to a small developmental window, perhaps less than 6 days after pollination, there may only be a short period of time where TE silencing is lost and TE activation can occur, leading to new TE insertions in the early embryo. Overall, our results show that TE presence/absence variants between wild Arabidopsis accessions can be linked to many DNA methylation changes previously observed in the population, and can have important consequences upon nearby gene expression. Furthermore, the differential TE content between parents can lead to DNA methylation changes in the early embryo, and could lead to activation of these elements.

METHODS

TEPID development

Mapping

FASTQ files are mapped to the reference genome using the 'tepid-map' algorithm (Fig. 1A). This first calls bowtie2 (Langmead and Salzberg 2012) with the following options: '--local', '--dovetail', '--fr', '-R5', '-N1'. Soft-clipped and unmapped reads are extracted using Samblaster (Faust and Hall 2014), and remapped using the split read mapper Yaha (Faust and Hall 2012), with the following options: '-L 11', '-H 2000', '-M 15', '-osh'. Split reads are extracted from the Yaha alignment using Samblaster (Faust and Hall 2014). Alignments are then converted to bam format, sorted, and indexed using samtools (Li et al. 2009).

TE variant discovery

The 'tepid-discover' algorithm examines mapped bam files generated by the 'tepid-map' step to identify TE presence/absence variants with respect to the reference genome. Firstly, mean sequencing coverage, mean library insert size, and standard deviation of the library insert size is estimated. Discordant read pairs are then extracted, defined as mate pairs that map more than 4 standard deviations from the mean insert size from one another, or on separate chromosomes.

To identify TE insertions with respect to the reference genome, split read alignments are first filtered to remove reads where the distance between split mapping loci is less than 5 kb, to remove split reads due to small indels, or split reads with a mapping quality (MAPQ) less than 5. Split and discordant read mapping coordinates are then intersected using pybedtools (Dale et al. 2011; Quinlan and Hall 2010) with the Col-0 reference TE annotation, requiring 80% overlap between TE and read mapping coordinates. To determine putative TE insertion sites, regions are then identified that contain independent discordant read pairs aligned in an orientation facing one another at the insertion site, with their mate pairs intersecting with the same TE (Fig. 1A). The total number of split and discordant reads intersecting the insertion site and the TE is then calculated, and a TE insertion predicted where the combined number of reads is greater than a threshold determined by the average sequencing depth over the whole genome (1/10 coverage if coverage is greater than 10, otherwise a minimum of 2 reads). Alternatively, in the absence of discordant reads mapped in orientations facing one another, the required total number of split and discordant reads at the insertion site linked to the inserted TE is set higher, requiring twice as many reads.

To identify TE absence variants with respect to the reference genome, split and discordant reads separated >20 kb from one another are first removed, as 99.9% of Arabidopsis TEs are shorter than 20 kb, and this removes split reads due to larger structural variants not related to TE diversity (Fig. S4A). Col-0 reference annotation TEs that are located within the genomic region spanned by the split and discordant reads are then identified. TE absence variants are predicted where at least 80% of the TE sequence is spanned by a split or discordant read, and the sequencing depth within the spanned region is <10% the sequencing depth of the 2 kb flanking sequence, and there are a minimum number of split and discordant reads present, determined by the sequencing depth (1/10 coverage; Fig. 1A). A threshold of 80% TE sequence spanned by split or discordant reads is used, as opposed to 100%, to account for misannotation of TE sequence boundaries in the Col-0 reference TE annotation, as well as TE fragments left behind by DNA TEs during cut-paste transposition (TE footprints) that may affect the mapping of reads around annotated TE borders (Plasterk 1991). This was found to improve TE absence detection using simulated data. Furthermore, the coverage within the spanned region may be more than 10% that of the flanking sequence, but in such cases twice as many split and discordant reads are required. If multiple TEs are spanned by the split and discordant reads, and the above requirements are met, multiple TEs in the same region can be identified as absent with respect to the reference genome. Absence variants in non-Col-0 accessions are subsequently recategorized as TE insertions present in the Col-0 genome but absent from a given wild accession.

TE variant refinement

Once TE insertions are identified using the 'tepid-map' and 'tepid-discover' algorithms, these variants can be refined if multiple related samples are analyzed. The 'tepid-refine' algorithm is designed to interrogate regions of the genome in which a TE insertion was discovered in other samples but not the sample in question, and check for evidence of that TE insertion in the sample using lower read count thresholds compared to the 'tepid-discover' step. In this way, the refine step leverages TE variant information for a group of related samples to reduce false negative calls within the group. This distinguishes TEPID from other similar methods for TE variant discovery utilizing short sequencing reads. A file containing the coordinates of each insertion, and a list of sample names containing the TE insertion must be provided to the 'tepid-refine' algorithm, which this can be generated using the 'merge_insertions.py' script included in the TEPID package. Each sample is examined in regions where there was a TE insertion identified in another sample in the group. If there is a sequencing breakpoint within this region (no continuous read coverage spanning the region), split reads mapped to this region will be extracted from the alignment file and their coordinates intersected with the TE reference annotation. If there are split reads present at the variant site that are linked to the same TE as was identified as an insertion at that location, this TE insertion is recorded in a new file as being present in the sample in question. If there is no sequencing coverage in the queried region for a sample, an "NA" call is made indicating that it is unknown whether the particular sample contains the TE insertion or not.

While the above description relates specifically to use of TEPID for identification of TE variants in Arabidopsis in this study, this method can be also applied to other species, with the only prerequisite being the annotation of TEs in a reference genome and the availability of paired-end DNA sequencing data.

TE variant simulation

To test the sensitivity and specificity of TEPID, 100 TE insertions (50 copy-paste transpositions, 50 cut-paste transpositions) and 100 TE absence variants were simulated in the Arabidopsis genome using the RSVSim R package, version 1.7.2 (Bartenhagen and Dugas 2013), and synthetic reads generated from the modified genome at various levels of sequencing coverage using wgsim (Li et al. 2009) (https://github.com/lh3/wgsim). These reads were then used to calculate the true positive, false positive, and false negative TE variant discovery rates for TEPID at various sequencing depths, by running 'tepid-map' and 'tepid-discover' using the simulated reads with the default parameters (Fig. 1B).

L*er* TE analysis

Previously published 100 bp paired end sequencing data for L*er* (http://1001genomes.org/data/MPI/MPISchneeberger2011/releases/current/Ler-1/Reads/; (Schneeberger et al. 2011)) was downloaded and analyzed with the TEPID package to identify TE variants. Reads providing evidence for TE variants were then mapped to the *de novo* assembled L*er* genome (Chin et al. 2013). To determine whether reads mapped to homologous regions of the L*er* and Col-0 reference genome, the *de novo* assembled L*er* genome sequence between mate pair mapping locations in L*er* were extracted, with repeats masked using RepeatMasker with RepBase-derived libraries and the default parameters (version 4.0.5, http://www.repeatmasker.org). A blastn search was then conducted against the Col-0 genome using the following parameters: '-max-target-seqs 1', '-evalue 1e-6' (Camacho et al. 2009).

Coordinates of the top blast hit for each read location were then compared with the TE variant sites identified using those reads.

Arabidopsis TE variant discovery

We ran the TEPID, including the insertion refinement step, on previously published sequencing data for 216 different Arabidopsis populations (NCBI SRA SRA012474; Schmitz et al. 2013), mapping to the TAIR10 reference genome and using the TAIR9 TE annotation. The '--mask' option was also used to mask the mitochondrial and plastid genomes. We also ran TEPID using previously published transgenerational data for salt stress and control conditions (NCBI SRA SRP045804; Jiang et al. 2014), using the '--mask' option to mask mitochondrial and plastid genomes, and the '--strict' option for highly related samples.

TE variant / SNP comparison

SNP information for 216 Arabidopsis accessions was obtained from the 1001 genomes data center (http://1001genomes.org/data/Salk/releases/2013_24_01/; Schmitz et al. 2013). This was formatted into reference (Col-0 state), alternate, or NA calls for each SNP. Accessions with both TE variant information and SNP data were selected for analysis. Hierarchical clustering of accessions by SNPs as well as TE variants were used to identify essentially clonal accessions, as these would skew minor allele frequency calculations. A single representative from each cluster of similar accessions was kept, leading to a total of 187 accessions for comparison. For each TE variant with minor-allele-frequency greater than 3%, the nearest 300 upstream and 300 downstream SNPs with a minor-allele-frequency greater than 3% were selected. Pairwise genotype correlations (r^2 values) for all complete cases were obtained for SNP-SNP and SNP-TE variant states. r^2 values were then ordered by decreasing rank and a median SNP-SNP rank value was calculated. For each of the 600 ranked surrounding positions, the number of times the TE rank was greater than the SNP-SNP median rank was calculated as a relative 'age' metric of TE to SNP. TE variants with less than 200 ranks over the SNP-SNP median were classified as 'young' insertions. Mid-age TE variants had ranks between 200 and 400, while TE variants with greater than 400 ranks above their respective SNP-SNP median value were classified as 'old' variants.

PCR validations

Selection of accessions to be genotyped

To assess the accuracy of TE variant calls in accessions with a range of sequencing depths of coverage, we grouped accessions into quartiles based on sequencing depth of coverage and randomly selected a total of 14 accessions for PCR validations from these quartiles. DNA was extracted for these accessions using Edward's extraction protocol (Edwards et al. 1991), and purified prior to PCR using AMPure beads.

Selection of TE variants for validation and primer design

Ten TE insertion sites and 10 TE absence sites were randomly selected for validation by PCR amplification. Only insertions and absence variants that were variable in at least two of the fourteen accessions selected to be genotyped were considered. For insertion sites, primers were designed to span the predicted TE insertion site. For TE absence sites, two primer sets were designed; one primer set to span the TE, and another primer set with one primer annealing within the TE sequence predicted to be absent, and the other primer annealing in the flanking sequence (Fig. 1C). Primer sequences were designed that did not anneal to regions of the genome containing previously identified SNPs in any of the 216 accessions (Schmitz et al. 2013) or small insertions and deletions, identified using lumpy-sv with the default settings (Layer et al. 2014)(https://github.com/arq5x/lumpy-sv), had an annealing temperature close to 52ºC calculated based on nearest neighbor thermodynamics (MeltingTemp submodule in the SeqUtils python module; (Cock et al. 2009)), a GC content between 40% and 60%, and contained the same base repeated not more than four times in a row. Primers were aligned to the TAIR10 reference genome using bowtie2 (Langmead and Salzberg 2012) with the '-a' flag set to report all alignments, and those with more than 5 mapping locations in the genome were then removed.

PCR

PCR was performed with 10 ng of extracted, purified Arabidopsis DNA using Taq polymerase. PCR products were analyzed by agarose gel electrophoresis. Col-0 was used as a positive control, water was added to reactions as a negative control.

mRNA analysis

Processed mRNA data for 144 wild Arabidopsis accessions were downloaded from NCBI GEO GSE43858 (Schmitz et al. 2013). To find differential gene expression dependent on TE presence/absence variation, we first filtered TE variants to include only those where the TE variant was shared by at least 5 accessions with RNA data available, corresponding to a minor allele frequency above 3%. We then grouped accessions based on TE presence/absence variants, and performed a Mann-Whitney U test to determine differences in RNA transcript abundance levels between the groups. We used q-value estimation to correct for multiple testing, using the R qvalue package v2.2.2 with the following parameters: lambda = seq(0, 0.6, 0.05), smooth.df = 4 (Storey and Tibshirani 2003). Genes were defined as differentially expressed where there was a greater than 2 fold difference in expression between the groups, with a q-value less than 0.001. Gene ontology enrichment analysis was performed using DAVID (https://david.ncifcrf.gov/).

DNA methylation data analysis

Processed DNA methylation data for wild Arabidopsis accessions were downloaded from NCBI GEO GSE43857 (Schmitz et al. 2013). Weighted embryo DNA methylation data in 300 bp windows for Col-0 crosses with Cvi 6 days after pollination were downloaded from the Dryad Digital Repository; http://dx.doi.org/10.5061/dryad.gv536.2 (Gehring et al. 2014). Processed embryo DNA methylation data in 50 bp windows for crosses between Col-0 and L*er* 7-8 days after pollination were downloaded from NCBI GEO GSE38935 (Ibarra et al. 2012).

Small RNA data analysis

Normalized 21-24 nt smRNA read counts (reads per million reads mapped; RPM) in 300 bp windows for whole seed 6 days after pollination, for reciprocal crosses between Col-0, Cvi, and L*er* were downloaded from the Dryad Digital Repository; http://dx.doi.org/10.5061/dryad.gv536.2 (Gehring et al. 2014).

DATA ACCESS

TEPID source code can be accessed at https://github.com/ListerLab/TEPID. L*er* TE variants are available in Supplementary File 1. TE variants identified among the 216 wild Arabidopsis accessions resequenced by Schmitz et al. (2013) are available in Supplementary File 2.

ACKNOWLEDGMENTS

This work was supported by the Australian Research Council (ARC) Centre of Excellence program in Plant Energy Biology CE140100008 (J.B., R.L.). R.L. was supported by an ARC Future Fellowship (FT120100862) and Sylvia and Charles Viertel Senior Medical Research

Fellowship, and work in the laboratory of R.L. was funded by the Australian Research Council. T.S. was supported by the Jean Rogerson Postgraduate Scholarship. S.R.E. was supported by an Australian Research Council Discovery Early Career Research Award (DE150101206). We thank Robert J. Schmitz, Mathew G. Lewsey, Ronan C. O'Malley, and Ian Small for their critical reading of the manuscript. We also thank Kevin Murray for his helpful comments regarding the development of TEPID.

AUTHOR CONTRIBUTIONS

R.L. and T.S. designed the research project. R.L. and J.B. supervised research. T.S. developed and tested TEPID. J.C. performed PCR validations of TE variants. T.S. and S.R.E. performed bioinformatic analysis. R.L., T.S., J.B. and S.R.E. prepared the manuscript.

COMPETING FINANCIAL INTERESTS

The authors declare no competing financial interests.

REFERENCES

Aranzana MJ, Kim S, Zhao K, Bakker E, Horton M, Jakob K, Lister C, Molitor J, Shindo C, Tang C, et al. 2005. Genome-Wide Association Mapping in Arabidopsis Identifies Previously Known Flowering Time and Pathogen Resistance Genes. *PLoS Genetics* **1**: e60–9.

Bartenhagen C, Dugas M. 2013. RSVSim: an R/Bioconductor package for the simulation of structural variations. *Bioinformatics* **29**: 1679–1681.

Bingham PM, Kidwell MG, Rubin GM. 1982. The molecular basis of P-M hybrid dysgenesis: the role of the P element, a P-strain-specific transposon family. *Cell* **29**: 995–1004.

Blumenstiel JP, Hartl DL. 2005. Evidence for maternally transmitted small interfering RNA in the repression of transposition in Drosophila virilis. *Proc Natl Acad Sci USA* **102**: 15965–15970.

Bolger A, Scossa F, Bolger ME, Lanz C, Maumus F, Tohge T, Quesneville H, Alseekh S, Sørensen I, Lichtenstein G, et al. 2014. The genome of the stress-tolerant wild tomato species. *Nat Genet* **46**: 1034–1038.

Bundock P, Hooykaas P. 2005. An Arabidopsis hAT-like transposase is essential for plant development. *Nature* **436**: 282–284.

Calarco JP, Borges F, Donoghue MTA, Van Ex F, Jullien PE, Lopes T, Gardner R, Berger F, FeijO JA, Becker JD, et al. 2012. Reprogramming of DNA Methylation in Pollen Guides Epigenetic Inheritance via Small RNA. *Cell* **151**: 194–205.

Camacho C, Coulouris G, Avagyan V, Ma N, Papadopoulos J, Bealer K, Madden TL. 2009. BLAST+: architecture and applications. *BMC Bioinformatics* **10**: 421.

Cao J, Schneeberger K, Ossowski S, Günther T, Bender S, Fitz J, Koenig D, Lanz C, Stegle O, Lippert C, et al. 2011. Whole-genome sequencing of multiple Arabidopsis thaliana populations. *Nat Genet* **43**: 956–963.

Chin C-S, Alexander DH, Marks P, Klammer AA, Drake J, Heiner C, Clum A, Copeland A, Huddleston J, Eichler EE, et al. 2013. Nonhybrid, finished microbial genome assemblies from long-read SMRT sequencing data. *Nat Meth* **10**: 563–569.

Cock PJA, Antao T, Chang JT, Chapman BA, Cox CJ, Dalke A, Friedberg I, Hamelryck T, Kauff F, Wilczynski B, et al. 2009. Biopython: freely available Python tools for computational molecular biology and bioinformatics. *Bioinformatics* **25**: 1422–1423.

Cokus SJ, Feng S, Zhang X, Chen Z, Merriman B, Haudenschild CD, Pradhan S, Nelson SF, Pellegrini M, Jacobsen SE. 2008. Shotgun bisulphite sequencing of the Arabidopsis genome reveals DNA methylation patterning. *Nature* **452**: 215–219.

Dale RK, Pedersen BS, Quinlan AR. 2011. Pybedtools: a flexible Python library for manipulating genomic datasets and annotations. *Bioinformatics* **27**: 3423–3424.

Edwards K, Johnstone C, Thompson C. 1991. A simple and rapid method for the preparation of plant genomic DNA for PCR analysis. *Nucleic Acids Research* **19**: 1349.

Faust GG, Hall IM. 2014. SAMBLASTER: fast duplicate marking and structural variant read extraction. *Bioinformatics* **30**: 2503–2505.

Faust GG, Hall IM. 2012. YAHA: fast and flexible long-read alignment with optimal breakpoint detection. *Bioinformatics* **28**: 2417–2424.

Gehring M, Pignatta D, Erdmann RM, Bell GW, Scheer E. 2014. *Data from: Natural epigenetic polymorphisms lead to intraspecific variation in Arabidopsis gene imprinting*. Dryad Digital

Repository.

Gendrel AV, Lippman Z, Yordan C, Colot V, Martienssen RA. 2002. Dependence of heterochromatic histone H3 methylation patterns on the Arabidopsis gene DDM1. *Science* **297**: 1871–1873.

Hénaff E, Vives C, Desvoyes B, Chaurasia A, Payet J, Gutierrez C, Casacuberta JM. 2014. Extensive amplification of the E2F transcription factor binding sites by transposons during evolution of Brassica species. *The Plant Journal* **77**: 852–862.

Hénaff E, Zapata L, Casacuberta JM, Ossowski S. 2015. Jitterbug: somatic and germline transposon insertion detection at single-nucleotide resolution. *BMC Genomics* **16**: 1–16.

Hirochika H, Okamoto H, Kakutani T. 2000. Silencing of retrotransposons in Arabidopsis and reactivation by the ddm1 mutation. *The Plant Cell* **12**: 357–369.

Hsieh TF, Ibarra CA, Silva P, Zemach A, Eshed-Williams L, Fischer RL, Zilberman D. 2009. Genome-Wide Demethylation of Arabidopsis Endosperm. *Science* **324**: 1451–1454.

Ibarra CA, Feng X, Schoft VK, Hsieh T-F, Uzawa R, Rodrigues JA, Zemach A, Chumak N, Machlicova A, Nishimura T, et al. 2012. Active DNA demethylation in plant companion cells reinforces transposon methylation in gametes. *Science* **337**: 1360–1364.

Ito H, Gaubert H, Bucher E, Mirouze M, Vaillant I, Paszkowski J. 2011. An siRNA pathway prevents transgenerational retrotransposition in plants subjected to stress. *Nature* **472**: 115–119.

Jeddeloh JA, Stokes TL, Richards EJ. 1999. Maintenance of genomic methylation requires a SWI2/SNF2-like protein. *Nat Genet* **22**: 94–97.

Jiang C, Mithani A, Belfield EJ, Mott R, Hurst LD, Harberd NP. 2014. Environmentally responsive genome-wide accumulation of de novo Arabidopsis thaliana mutations and epimutations. *Genome Research* **24**: 1821–1829.

Josefsson C, Dilkes B, Comai L. 2006. Parent-dependent loss of gene silencing during interspecies hybridization. *Current Biology* **16**: 1322–1328.

Jullien PE, Susaki D, Yelagandula R, Higashiyama T, Berger F. 2012. DNA Methylation Dynamics during Sexual Reproduction in Arabidopsis thaliana. *Curr Biol* **22**: 1825–1830.

Katoh A, Uenohara K, Akita M, Hashimoto T. 2006. Early steps in the biosynthesis of NAD in Arabidopsis start with aspartate and occur in the plastid. *Plant Physiology* **141**: 851–857.

Kawashima T, Berger F. 2014. Epigenetic reprogramming in plant sexual reproduction. *Nature Reviews Genetics* **15**: 613–624.

Langmead B, Salzberg SL. 2012. Fast gapped-read alignment with Bowtie 2. *Nat Meth* **9**: 357–359.

Layer RM, Chiang C, Quinlan AR, Hall IM. 2014. LUMPY: a probabilistic framework for structural variant discovery. *Genome Biology* **15**: R84.

Li H, Handsaker B, Wysoker A, Fennell T, Ruan J, Homer N, Marth G, Abecasis G, Durbin R, 1000 Genome Project Data Processing Subgroup. 2009. The Sequence Alignment/Map format and SAMtools. *Bioinformatics* **25**: 2078–2079.

Lippman Z, Gendrel A-V, Black M, Vaughn MW, Dedhia N, McCombie WR, Lavine K, Mittal V, May B, Kasschau KD, et al. 2004. Role of transposable elements in heterochromatin and epigenetic control. *Nature* **430**: 471–476.

Lister R, O'Malley RC, Tonti-Filippini J, Gregory BD, Berry CC, Millar AH, Ecker JR. 2008. Highly integrated single-base resolution maps of the epigenome in Arabidopsis. *Cell* **133**: 523–536.

Makarevitch I, Waters AJ, West PT, Stitzer M, Hirsch CN, Ross-Ibarra J, Springer NM. 2015. Transposable Elements Contribute to Activation of Maize Genes in Response to Abiotic Stress. *PLoS Genetics* **11**: e1004915.

Martienssen RA. 2010. Heterochromatin, small RNA and post-fertilization dysgenesis in allopolyploid and interploid hybrids of Arabidopsis. *New Phytologist* **186**: 46–53.

Matzke MA, Mosher RA. 2014. RNA-directed DNA methylation: an epigenetic pathway of increasing complexity. *Nature Reviews Genetics* **15**: 394–408.

Mirouze M, Reinders J, Bucher E, Nishimura T, Schneeberger K, Ossowski S, Cao J, Weigel D, Paszkowski J, Mathieu O. 2009. Selective epigenetic control of retrotransposition in Arabidopsis. *Nature* **461**: 427–430.

Miura A, Yonebayashi S, Watanabe K, Toyama T. 2001. Mobilization of transposons by a mutation abolishing full DNA methylation in Arabidopsis. *Nature* **411**: 212–214.

Mosher RA, Melnyk CW, Kelly KA, Dunn RM, Studholme DJ, Baulcombe DC. 2009. Uniparental expression of PolIV-dependent siRNAs in developing endosperm of Arabidopsis. *Nature* **460**: 283–286.

Pignatta D, Erdmann RM, Scheer E, Picard CL, Bell GW, Gehring M. 2014. Natural epigenetic polymorphisms lead to intraspecific variation in Arabidopsis gene imprinting. *eLife* **3**: e03198.

Plasterk R. 1991. The Origin of Footprints of the Tc1 Transposon of Caenorhabditis elegans. *EMBO* **10**: 1919–1925.

Quinlan AR, Hall IM. 2010. BEDTools: a flexible suite of utilities for comparing genomic features. *Bioinformatics* **26**: 841–842.

Richards EJ. 2006. Inherited epigenetic variation - revisiting soft inheritance. *Nature Reviews Genetics* **7**: 395–U2.

Robb S, Lu L, Valencia E, Burnette JM. 2013. The use of RelocaTE and unassembled short reads to produce high-resolution snapshots of transposable element generated diversity in rice. *G3: Genes| Genomes| Genetics*.

Saze H, Scheid OM, Paszkowski J. 2003. Maintenance of CpG methylation is essential for epigenetic inheritance during plant gametogenesis. *Nat Genet* **34**: 65–69.

Schmitz RJ, Schultz MD, Urich MA, Nery JR, Pelizzola M, Libiger O, Alix A, McCosh RB, Chen H, Schork NJ, et al. 2013. Patterns of population epigenomic diversity. *Nature* **495**: 193–198.

Schneeberger K, Ossowski S, Ott F, Klein JD, Wang X, Lanz C, Smith LM, Cao J, Fitz J, Warthmann N, et al. 2011. Reference-guided assembly of four diverse Arabidopsis thaliana genomes. *Proc Natl Acad Sci USA* **108**: 10249–10254.

Slotkin RK, Vaughn M, Borges F, TanurdZiC M, Becker JD, FeijO JA, Martienssen RA. 2009. Epigenetic reprogramming and small RNA silencing of transposable elements in pollen. *Cell* **136**: 461–472.

Storey JD, Tibshirani R. 2003. Statistical significance for genomewide studies. *Proc Natl Acad*

Sci USA **100**: 9440–9445.

Stroud H, Greenberg MVC, Feng S, Bernatavichute YV, Jacobsen SE. 2013. Comprehensive analysis of silencing mutants reveals complex regulation of the Arabidopsis methylome. *Cell* **152**: 352–364.

Sullivan AM, Arsovski AA, Lempe J, Bubb KL, Weirauch MT, Sabo PJ, Sandstrom R, Thurman RE, Neph S, Reynolds AP, et al. 2014. Mapping and dynamics of regulatory DNA and transcription factor networks in A. thaliana. *Cell* **8**: 2015–2030.

Thung DT, de Ligt J, Vissers LE, Steehouwer M, Kroon M, de Vries P, Slagboom EP, Ye K, Veltman JA, Hehir-Kwa JY. 2014. Mobster: accurate detection of mobile element insertions in next generation sequencing data. 1–11.

Vitte C, Fustier M-A, Alix K, Tenaillon MI. 2014. The bright side of transposons in crop evolution. *Briefings in Functional Genomics* **13**: 276–295.

Wang G, Ellendorff U, Kemp B, Mansfield JW, Forsyth A, Mitchell K, Bastas K, Liu C-M, Woods-Tör A, Zipfel C, et al. 2008. A genome-wide functional investigation into the roles of receptor-like proteins in Arabidopsis. *Plant Physiology* **147**: 503–517.

Wicker T, Sabot F, Hua-Van A, Bennetzen JL, Capy P, Chalhoub B, Flavell A, Leroy P, Morgante M, Panaud O, et al. 2007. A unified classification system for eukaryotic transposable elements. *Nature Reviews Genetics* **8**: 973–982.

Zemach A, Kim MY, Hsieh P-H, Coleman-Derr D, Eshed-Williams L, Thao K, Harmer SL, Zilberman D. 2013. The Arabidopsis Nucleosome Remodeler DDM1 Allows DNA Methyltransferases to Access H1-Containing Heterochromatin. *Cell* **153**: 193–205.

Zhang X, Yazaki J, Sundaresan A, Cokus S, Chan SWL, Chen H, Henderson IR, Shinn P, Pellegrini M, Jacobsen SE, et al. 2006. Genome-wide High-Resolution Mapping and Functional Analysis of DNA Methylation in Arabidopsis. *Cell* **126**: 1189–1201.

Zilberman D, Gehring M, Tran RK, Ballinger T, Henikoff S. 2007. Genome-wide analysis of Arabidopsis thaliana DNA methylation uncovers an interdependence between methylation and transcription. *Nat Genet* **39**: 61–69.

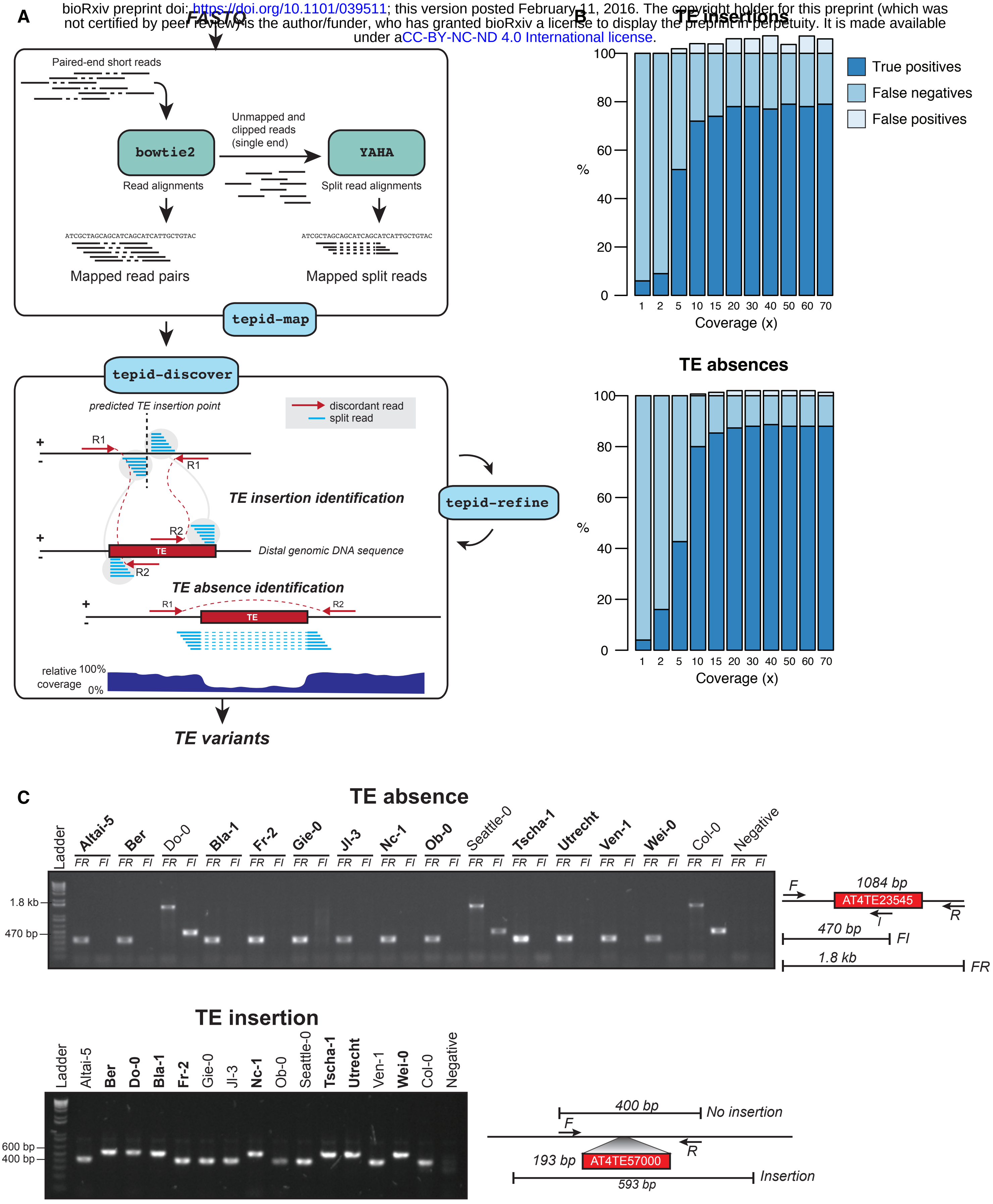

D

	True positives	False positives	False negatives
Absences	77.10%	9.16%	13.74%
Insertions	70.71%	9.29%	20.00%

Figure 1. Design and testing of the TE variant discovery pipeline

(A) Principle of TE variant discovery using split and discordant read mapping positions. Paired end reads are first mapped to the reference genome using Bowtie2 (Langmead and Salzberg 2012). Soft-clipped or unmapped reads are then extracted from the alignment and re-mapped using Yaha, a split read mapper (Faust and Hall 2012). All read alignments are then used by TEPID to discover TE variants relative to the reference genome, in the ‘tepid-discover’ step. When analyzing groups of related samples, these variants can be further refined using the ‘tepid-refine’ step, which examines in more detail the genomic regions where there was a TE variant identified in another sample, and calls the same variant for the sample in question using lower read count thresholds as compared to the ‘tepid-discover’ step, in order to reduce false negative variant calls within a group of related samples.

(B) Testing of the TEPID pipeline using simulated TE variants in the Arabidopsis Col-0 genome (TAIR10), for a range of sequencing coverage levels.

(C) PCR validation examples for TE presence/absence variant predictions. Accessions that were predicted to contain a TE insertion or TE absence are marked in bold. For the example TE absence variant, two primer sets were used; forward (F) and reverse (R) or internal (I). Accessions with a TE absence will not produce the FI band and produce a shorter FR product, with the change in size matching the size of the deleted TE. For the example TE insertion, one primer set was used, spanning the TE insertion site. A band shift of approximately 200 bp can be seen, corresponding to the size of the inserted TE.

(D) Summary table of PCR validation results for TE variants.

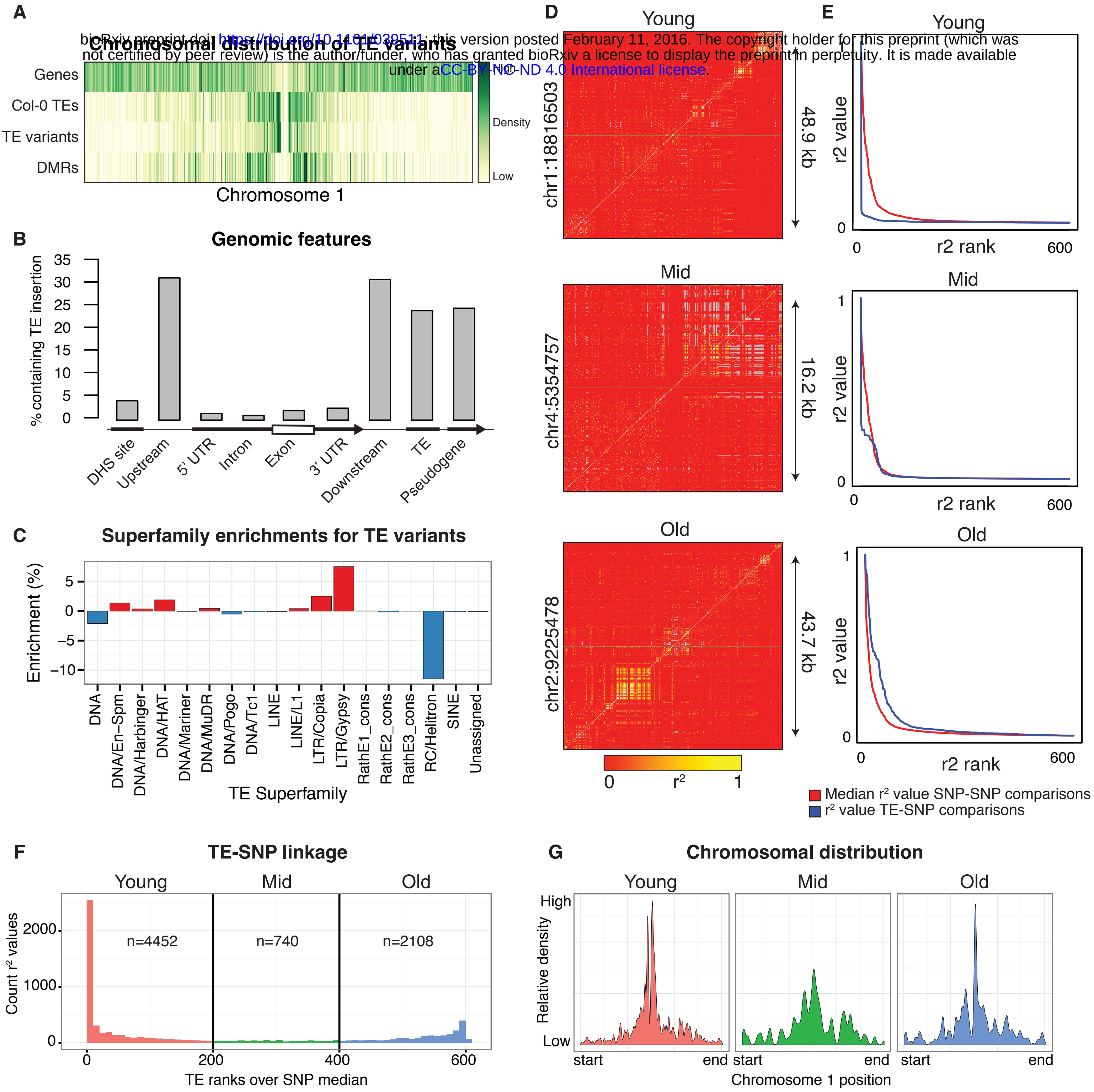
A
Chromosomal distribution of TE variants
Genes
Col-0 TEs
TE variants
DMRs
Density
Low
Chromosome 1
B
Genomic features
% containing TE insertion
35
30
25
20
15
10
5
0
DHS site
Upstream
5' UTR
Intron
Exon
3' UTR
Downstream
TE
Pseudogene
C
Superfamily enrichments for TE variants
Enrichment (%)
5
0
−5
−10
DNA
DNA/En−Spm
DNA/Harbinger
DNA/HAT
DNA/Mariner
DNA/MuDR
DNA/Pogo
DNA/Tc1
LINE
LINE/L1
LTR/Copia
LTR/Gypsy
RathE1_cons
RathE2_cons
RathE3_cons
RC/Helitron
SINE
Unassigned
TE Superfamily
D
Young
chr1:18816503
48.9 kb
Mid
chr4:5354757
16.2 kb
Old
chr2:9225478
43.7 kb
0
r²
1
E
Young
r2 value
1
0
0
r2 rank
600
Mid
r2 value
1
0
0
r2 rank
600
Old
r2 value
1
0
0
r2 rank
600
🟥 Median r² value SNP-SNP comparisons
🟦 r² value TE-SNP comparisons
F
TE-SNP linkage
Young
Mid
Old
Count r² values
2000
1000
0
n=4452
n=740
n=2108
0
200
400
600
TE ranks over SNP median
G
Chromosomal distribution
Young
Mid
Old
High
Relative density
Low
start
end
start
end
start
end
Chromosome 1 position

Figure 2. Extensive novel genetic diversity uncovered by TE variant analysis

(A) Distribution of identified TE variants on chromosome 1, with distributions of all Col-0 genes, Col-0 TEs, and population DMRs.

(B) Frequency of TE variants at different genomic features.

(C) Enrichment and depletion of TE variants categorized by TE superfamily compared to the expected frequency due to genomic occurrence.

(D) r^2 correlation matrices for individual representative young, mid, and old TE variants.

(E) Rank order plots for individual representative young, mid, and old TE variants (matching those shown in D). Red line indicates the median r^2 value for each rank across SNP-based values. Blue line indicates r^2 values for TE-SNP comparisons.

(F) Histogram of the number of TE r^2 ranks (0-600) that are above the SNP-based median r^2 value for testable TE variants. TE variants with <200 ranks over the SNP median were classified as “young” elements, as they are not yet linked to the surrounding SNPs. TE variants with 200-400 ranks over the SNP median were classified as “mid” aged. TE variants with >400 ranks over the SNP median were classified as “old” elements, as they were linked to the surrounding SNPs.

(G) Chromosomal distribution of TE variants by age.

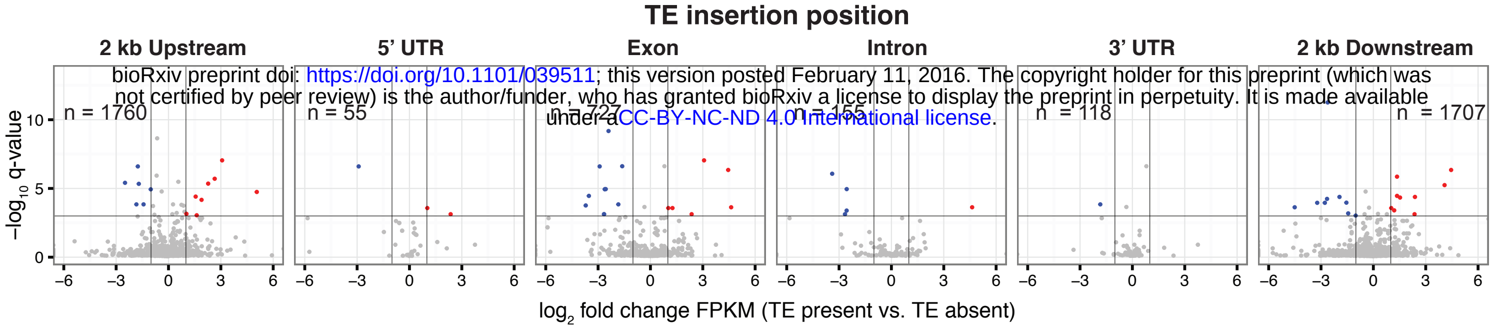
TE insertion position
2 kb Upstream
5' UTR
Exon
Intron
3' UTR
2 kb Downstream
n = 1760
n = 55
n = 727
n = 155
n = 118
n = 1707
$-\log_{10}$ q-value
0
5
10
−6
−3
0
3
6
$\log_2$ fold change FPKM (TE present vs. TE absent)

Figure 3. Differential transcript abundance associated with genic TE variant presence/absence

Volcano plots showing transcript abundance differences for genes associated with TE insertion variants at different positions, indicated in the plot titles. Genes with significantly different transcript abundance in accessions with a TE insertion compared to accessions without a TE insertion are colored blue (lower transcript abundance in accessions containing TE insertion) or red (higher transcript abundance in accessions containing TE insertion). Vertical lines indicate ±2 fold change in FPKM.

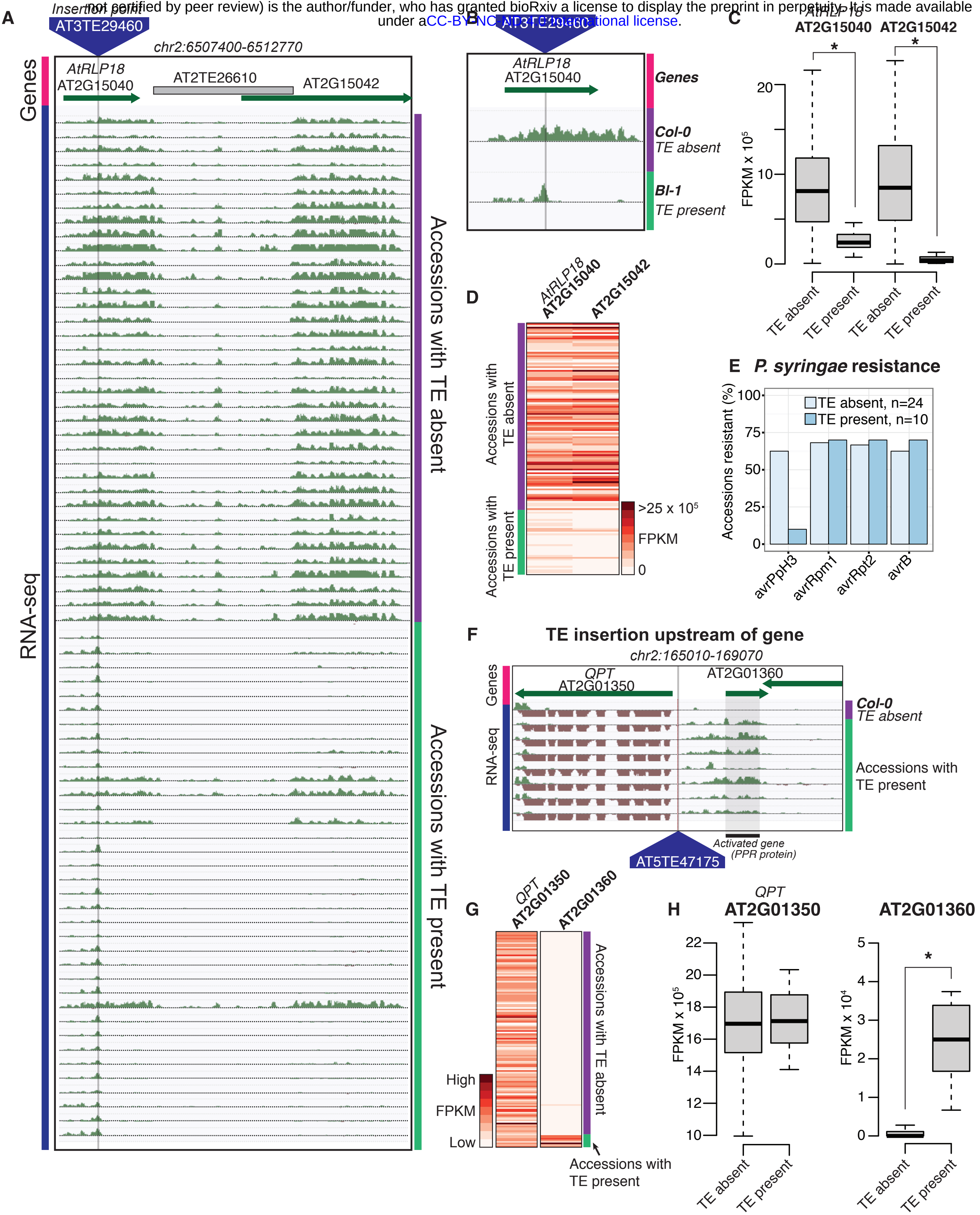
A
Insertion point
AT3TE29460
chr2:6507400-6512770
Genes
AtRLP18
AT2G15040
AT2TE26610
AT2G15042
RNA-seq
Accessions with TE absent
Accessions with TE present
B
AT3TE29460
AtRLP18
AT2G15040
Genes
Col-0
TE absent
Bl-1
TE present
C
AtRLP18
AT2G15040
AT2G15042
*
*
FPKM x 10^5
20
10
0
TE absent
TE present
TE absent
TE present
D
AtRLP18
AT2G15040
AT2G15042
Accessions with TE absent
Accessions with TE present
>25 x 10^5
FPKM
0
E
P. syringae resistance
Accessions resistant (%)
100
75
50
25
0
TE absent, n=24
TE present, n=10
avrPphB
avrRpm1
avrRpt2
avrB
F
TE insertion upstream of gene
chr2:165010-169070
Genes
RNA-seq
QPT
AT2G01350
AT2G01360
Col-0
TE absent
Accessions with TE present
AT5TE47175
Activated gene
(PPR protein)
G
QPT
AT2G01350
AT2G01360
High
FPKM
Low
Accessions with TE absent
Accessions with TE present
H
QPT
AT2G01350
AT2G01360
FPKM x 10^5
22
20
18
16
14
12
10
FPKM x 10^4
5
4
3
2
1
0
*
TE absent
TE present
TE absent
TE present

Figure 4. Effects of TE variants on local gene expression

(A) Genome browser representation of RNA-seq data for genes *AtRLP18* (AT2G15040) and a leucine-rich repeat family protein (AT2G15042) for all accessions containing a TE insertion within the exon of the gene *AtRLP18*, and for a random subset of accessions not containing the TE insertion within the exon of *AtRLP18*.

(B) Magnified view of the TE insertion variant within the *AtRLP18* exon.

(C) Boxplots comparing transcript abundance of *AtRLP18* and AT2G15042 in accessions with and without the TE insertion in the *AtRLP18* exon. Asterisk indicates statistical significance ($p < 5.8 \times 10^{-10}$; Mann-Whitney U test). Boxes represent the interquartile range (IQR) from quartile 1 to quartile 3. Boxplot upper whiskers represent the maximum value, or the upper value of the quartile 3 plus 1.5 times the IQR (whichever is smaller). Boxplot lower whisker represents the minimum value, or the lower value of the quartile 1 minus 1.5 times the IQR (whichever is larger).

(D) Heatmap showing *AtRLP18* and AT2G15042 RNA-seq FPKM values for all accessions.

(E) Percentage of accessions with resistance to *Pseudomonas syringae* transformed with different *avr* genes, for accessions containing or not containing a TE insertion in *AtRLP18.*

(F) Genome browser representation of RNA-seq data for a PPR protein-encoding gene (AT2G01360) and *QPT* (AT2G01350), showing transcript abundance for these genes in accessions containing a TE insertion variant in the upstream region of these genes.

(G) Heatmap representation of RNA-seq FPKM values for *QPT* and a gene encoding a PPR protein (AT2G01360), for all accessions. Note that scales are different for the two heatmaps, due to the higher transcript abundance of *QPT* compared to AT2G01360. Scale maximum for AT2G01350 is 3.1×10^5, and for AT2G01360 is 5.9×10^4.

(H) Boxplots showing RNA-seq FPKM differences for *QPT* and AT2G01360 associated with presence/absence of a TE variant in the gene upstream region. Asterisk indicates statistical significance ($p < 1.8 \times 10^{-7}$, Mann-Whitney U test). Boxplots were constructed as for C.

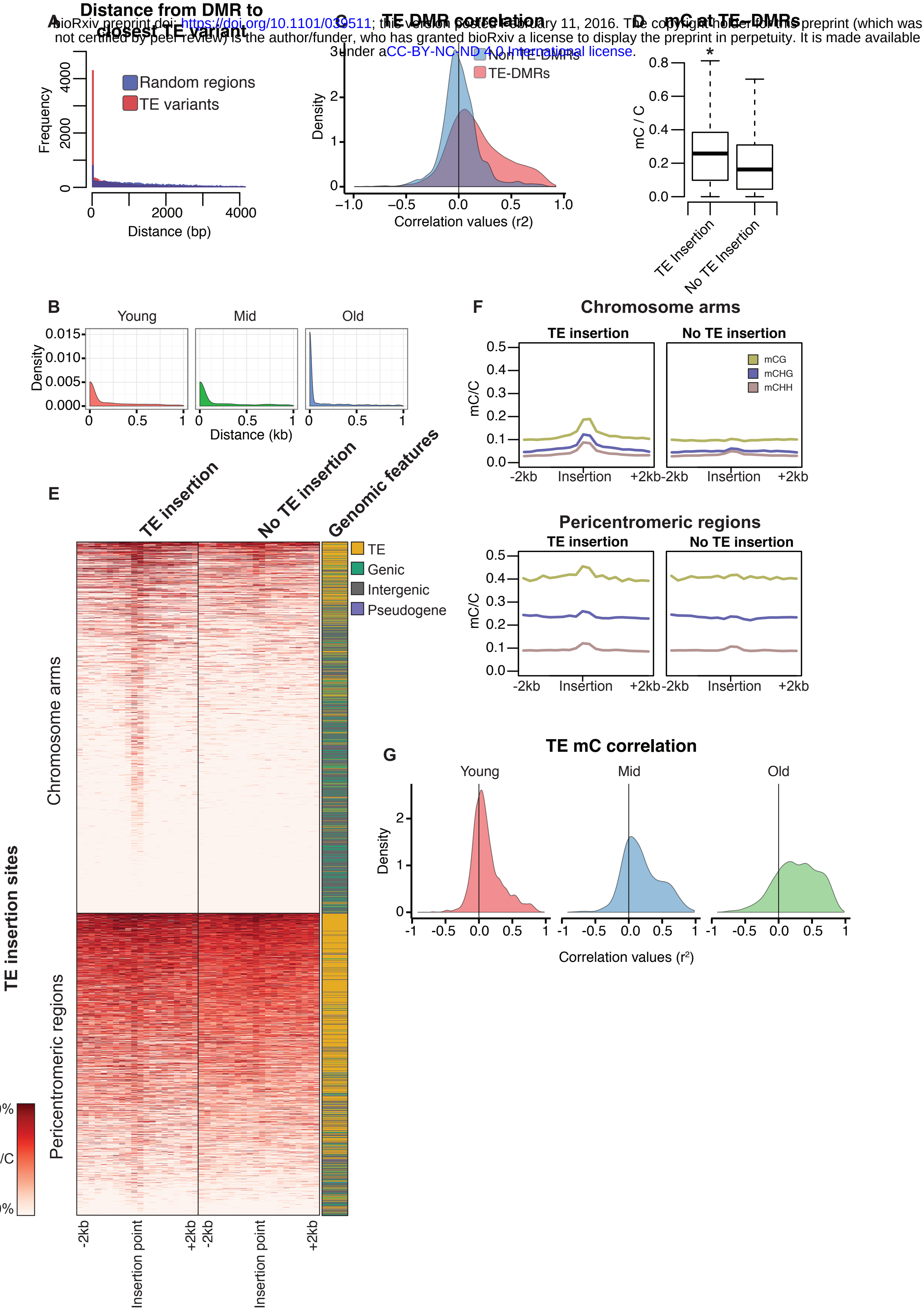
A
Distance from DMR to closest TE variant
Frequency
0
2000
4000
Random regions
TE variants
0
2000
4000
Distance (bp)
C
TE-DMR correlation
Density
0
1
2
3
Non TE-DMRs
TE-DMRs
−1.0
−0.5
0.0
0.5
1.0
Correlation values (r2)
D
mC at TE-DMRs
mC / C
0.0
0.2
0.4
0.6
0.8
*
TE Insertion
No TE Insertion
B
Young
Mid
Old
Density
0.000
0.005
0.010
0.015
0
0.5
1
Distance (kb)
F
Chromosome arms
TE insertion
No TE insertion
mC/C
0.0
0.1
0.2
0.3
0.4
0.5
mCG
mCHG
mCHH
-2kb
Insertion
+2kb
Pericentromeric regions
TE insertion
No TE insertion
mC/C
0.0
0.1
0.2
0.3
0.4
0.5
-2kb
Insertion
+2kb
E
TE insertion
No TE insertion
Genomic features
TE
Genic
Intergenic
Pseudogene
TE insertion sites
Chromosome arms
Pericentromeric regions
>50%
mC/C
0%
-2kb
Insertion point
+2kb
G
TE mC correlation
Young
Mid
Old
Density
0
1
2
-1
-0.5
0.0
0.5
1
Correlation values (r²)

Figure 5. TE variants are associated with DNA methylation changes

(A) Distance from each population DMR to closest TE variant (red), compared with a set of randomly selected regions of the genome, of the same size as all TE variants (blue).

(B) Density of distance measurements between population DMRs and the closest TE variant, grouped by age classification of TE variant.

(C) Density of Pearson correlation values between DNA methylation levels at population DMRs and the presence/absence of the nearest TE variants. Pearson correlation values for population DMRs within 1 kb of a TE variant (TE-DMRs) are shown in red, while values for population DMRs further than 1 kb from a TE variant (non TE-DMRs) are shown in blue.

(D) Boxplot showing DNA methylation levels at TE-DMRs for accessions containing the TE insertion and accessions not containing the TE insertion. Asterisk indicates statistical significance ($p < 2.2 \times 10^{-16}$, Welch's t-test). Boxplots were constructed as for Fig. 4C.

(E) DNA methylation levels in 200 bp windows ± 2 kb from TE insertion sites, for accessions with and without the TE insertion. Heatmap is separated into in regions of the genome less than 3 Mb from a centromere (pericentromeric regions) or greater than 3 Mb from a centromere (chromosome arms), and sorted by total DNA methylation at each locus.

(F) Average DNA methylation levels in mCG, mCHG and mCHH contexts in regions surrounding TE insertion variant sites for pericentromeric insertions and insertions in the euchromatic chromosome arms.

(G) Density of Pearson correlation values between DNA methylation levels in 200 bp regions flanking TE variant sites and the presence/absence of the TE variant, separated by TE age groups. Only TEs that were able to be assigned an age group are shown (total 7,300; minor allele frequency >3%).

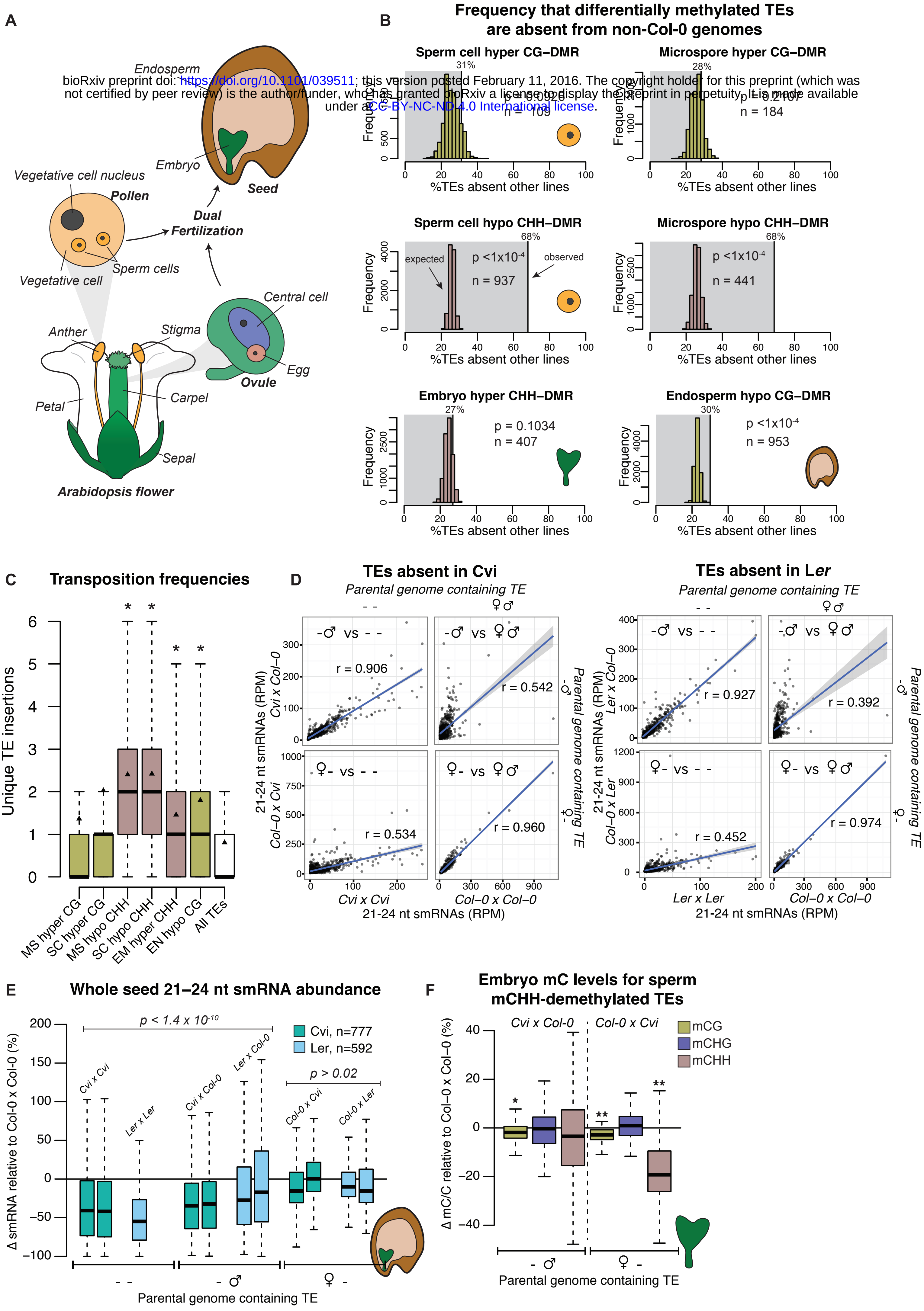
A
Endosperm
Embryo
Seed
Vegetative cell nucleus
Pollen
Dual Fertilization
Vegetative cell
Sperm cells
Central cell
Anther
Stigma
Egg
Ovule
Carpel
Petal
Sepal
Arabidopsis flower
B
Frequency that differentially methylated TEs are absent from non-Col-0 genomes
Sperm cell hyper CG−DMR
31%
p = 0.0926
n = 109
Microspore hyper CG−DMR
28%
p = 0.2167
n = 184
Sperm cell hypo CHH−DMR
68%
expected
observed
p <1x10-4
n = 937
Microspore hypo CHH−DMR
68%
p <1x10-4
n = 441
Embryo hyper CHH−DMR
27%
p = 0.1034
n = 407
Endosperm hypo CG−DMR
30%
p <1x10-4
n = 953
Frequency
%TEs absent other lines
0
20
40
60
80
100
C
Transposition frequencies
Unique TE insertions
0
1
2
3
4
5
6
*
MS hyper CG
SC hyper CG
MS hypo CHH
SC hypo CHH
EM hyper CHH
EN hypo CG
All TEs
D
TEs absent in Cvi
TEs absent in Ler
Parental genome containing TE
- -
♀♂
-♂ vs - -
-♂ vs ♀♂
♀- vs - -
♀- vs ♀♂
r = 0.906
r = 0.542
r = 0.534
r = 0.960
r = 0.927
r = 0.392
r = 0.452
r = 0.974
-♂
♀-
21-24 nt smRNAs (RPM)
Cvi x Col-0
Col-0 x Cvi
Ler x Col-0
Col-0 x Ler
Cvi x Cvi
Col−0 x Col−0
Ler x Ler
21-24 nt smRNAs (RPM)
E
Whole seed 21−24 nt smRNA abundance
Δ smRNA relative to Col-0 x Col-0 (%)
p < 1.4 x 10-10
p > 0.02
Cvi, n=777
Ler, n=592
Cvi x Cvi
Ler x Ler
Cvi x Col-0
Ler x Col-0
Col-0 x Cvi
Col-0 x Ler
200
150
100
50
0
−50
−100
- -
- ♂
♀ -
Parental genome containing TE
F
Embryo mC levels for sperm mCHH-demethylated TEs
Cvi x Col-0
Col-0 x Cvi
mCG
mCHG
mCHH
Δ mC/C relative to Col−0 x Col−0 (%)
40
20
0
−20
−40
*
**
- ♂
♀ -
Parental genome containing TE

Figure 6. Genetic differences between parents is associated with demethylation of transposable elements in hybrid progeny

(A) Diagram of the developing pollen, ovule, and seed. During dual fertilization, one sperm fertilizes the egg forming the embryo, while the other fertilizes the central cell to form the endosperm.

(B) Percentage of TEs differentially methylated in germline cell types that were absent in at least one non-Col-0 accession (shaded region) and expected percentage (histogram). 68% of TEs that lose mCHH in the sperm cell or microspore are absent from non-reference accessions, significantly more often than expected ($p < 1 \times 10^{-4}$, determined by resampling 10,000 times). Embryo DMRs are in comparison to aerial tissues, endosperm DMRs are in comparison to the embryo.

(C) Frequency of transposition for TEs differentially methylated in the microspore (MS), sperm cell (SC), embryo (EM) and endosperm (EN). Black triangles represent the mean number of unique TE insertion sites caused by elements in each list, asterisk indicates significance ($p < 1 \times 10^{-5}$, Welch's t-test). Boxplots were constructed as for Fig. 4C.

(D) Correlation between whole seed 21-24 nt smRNA levels (normalized reads per million values in 300 bp windows; RPM) for TEs present in maternal or paternal genomes only, compared with smRNA levels in crosses where the TE is present or absent in both parental genomes. Direction of each cross is represented on axes as *female x male*. TE variants are always present in the Col-0 genome and absent in the non-Col-0 genome. R values are Pearson's correlation coefficient.

(E) Whole seed 21-24 nt smRNA abundance (RPM, as for D) in TEs absent in Cvi for crosses between Cvi and Col-0, or absent in L*er* for crosses between L*er* and Col-0. Direction of each cross is represented as *female x male* on boxplot labels. Replicates are plotted side-by-side, p-values are the result of a Mann-Whitney U test using averaged replicate data. Boxplots were constructed as for Fig. 4C.

(F) Embryonic DNA methylation levels 6 days after pollination for Cvi-absent TEs that lose mCHH in sperm, following reciprocal crosses between Col-0 and Cvi. Boxplots were constructed as for Fig. 4C.

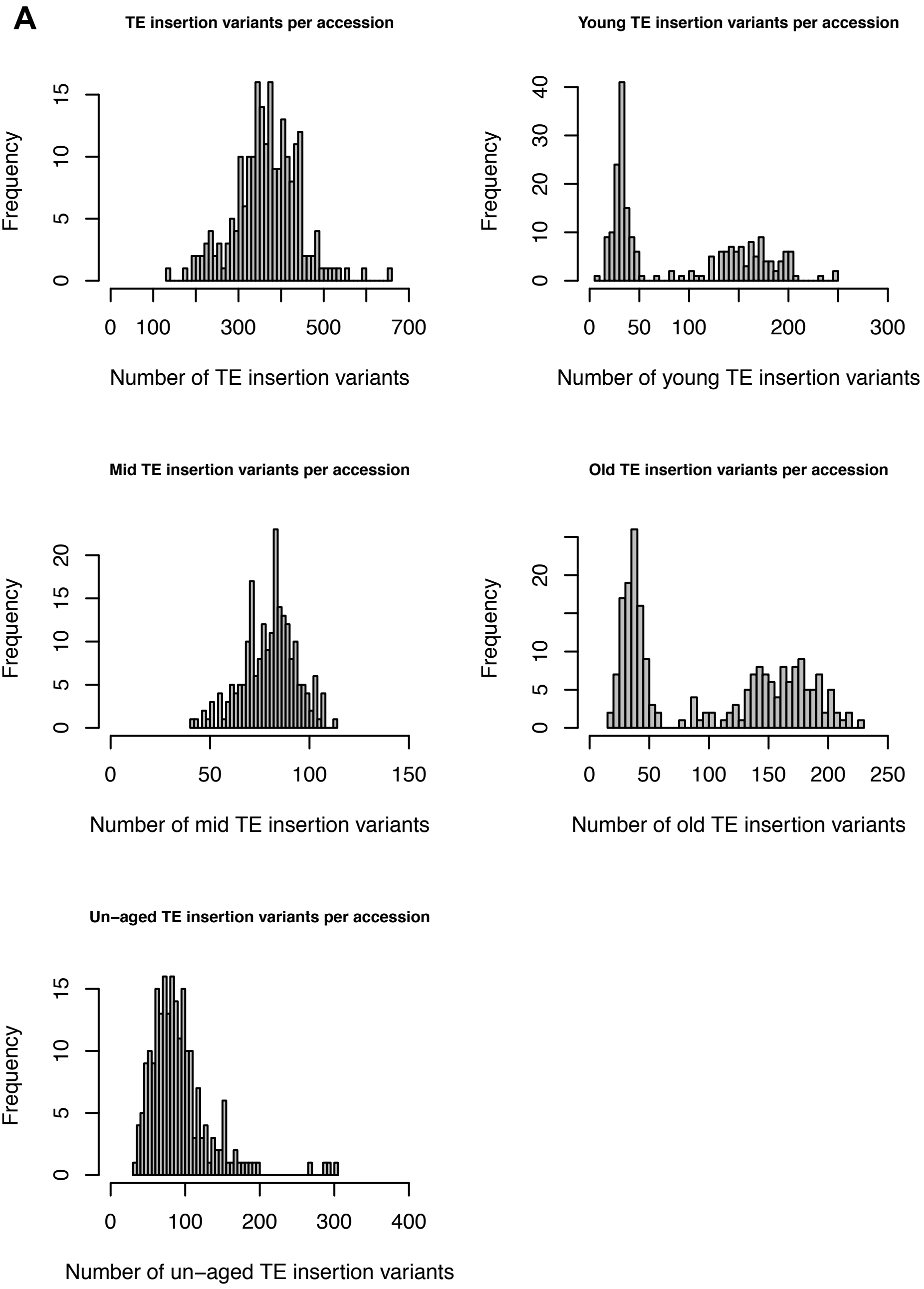
A
TE insertion variants per accession
Frequency
0
5
10
15
0
100
300
500
700
Number of TE insertion variants
Young TE insertion variants per accession
Frequency
0
10
20
30
40
0
50
100
200
300
Number of young TE insertion variants
Mid TE insertion variants per accession
Frequency
0
5
10
15
20
0
50
100
150
Number of mid TE insertion variants
Old TE insertion variants per accession
Frequency
0
5
10
20
0
50
100
150
200
250
Number of old TE insertion variants
Un−aged TE insertion variants per accession
Frequency
0
5
10
15
0
100
200
300
400
Number of un−aged TE insertion variants

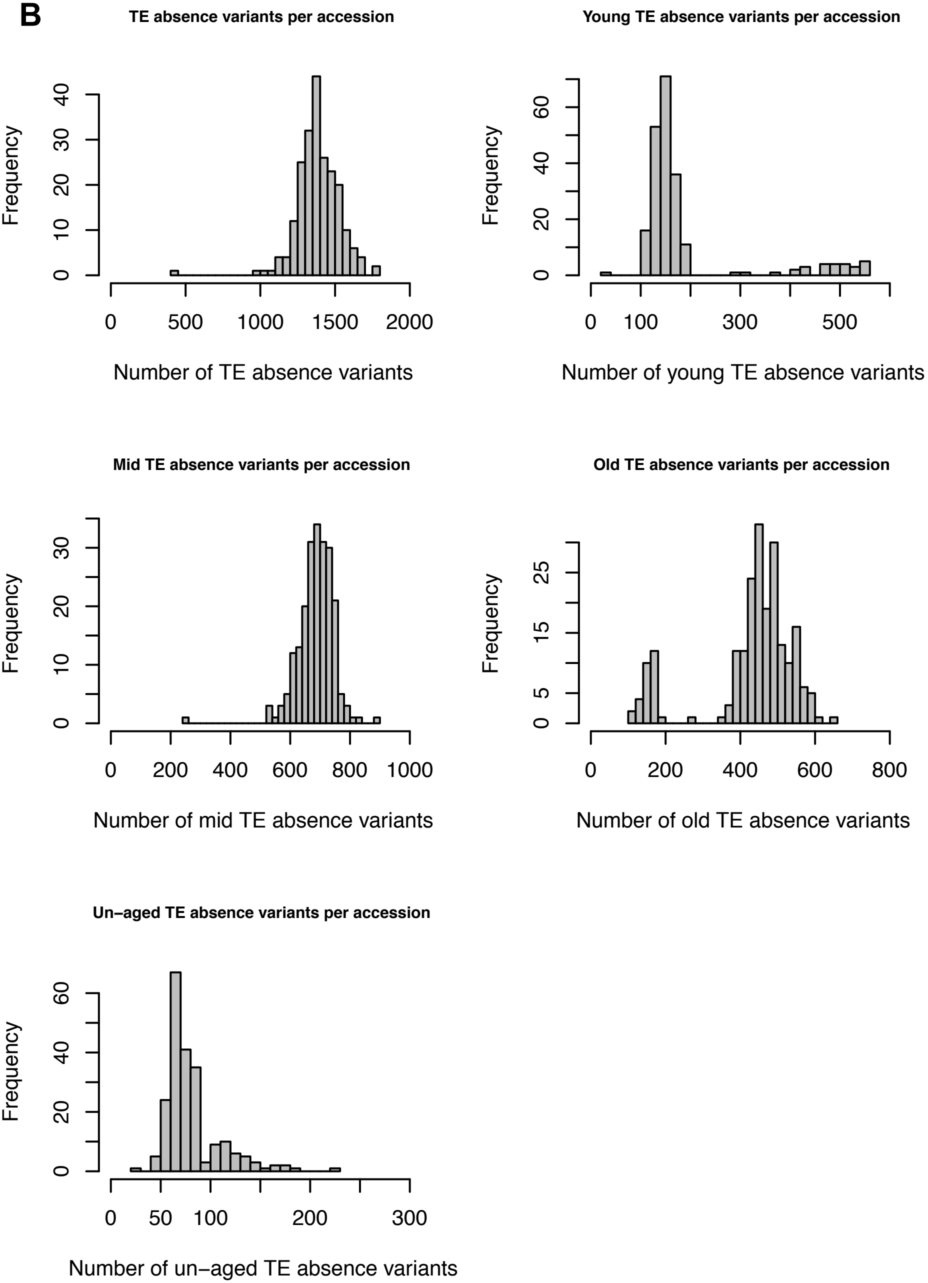
B
TE absence variants per accession
Frequency
0
10
20
30
40
0
500
1000
1500
2000
Number of TE absence variants
Young TE absence variants per accession
Frequency
0
20
40
60
0
100
300
500
Number of young TE absence variants
Mid TE absence variants per accession
Frequency
0
10
20
30
0
200
400
600
800
1000
Number of mid TE absence variants
Old TE absence variants per accession
Frequency
0
5
15
25
0
200
400
600
800
Number of old TE absence variants
Un−aged TE absence variants per accession
Frequency
0
20
40
60
0
50
100
200
300
Number of un−aged TE absence variants

Figure S1. Number of TE presence/absence variants identified for each wild accession.

(A) Histograms showing number of TE insertion variants identified for each accession, separated by all TE insertions, and the different TE insertion age classes.

(B) TE absence variants as for A.

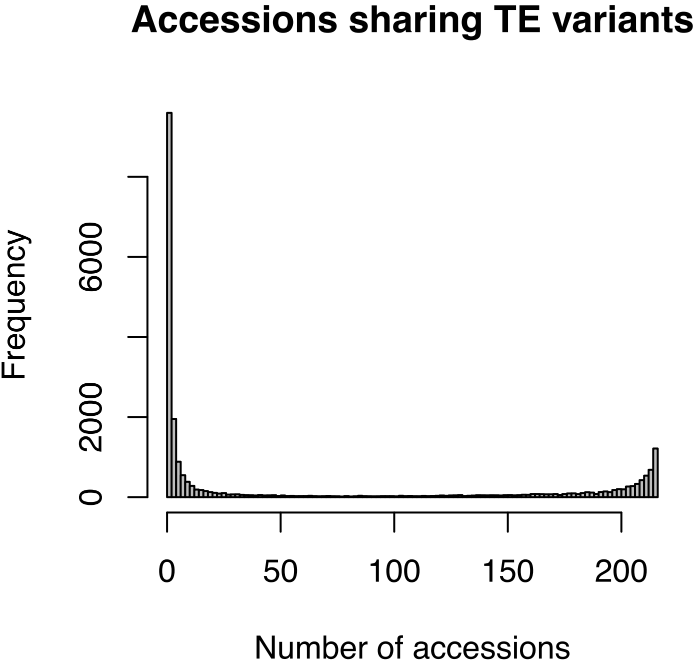
Accessions sharing TE variants
Frequency
0
2000
6000
0
50
100
150
200
Number of accessions

Figure S2. Histogram showing number of accessions sharing each TE variant identified.

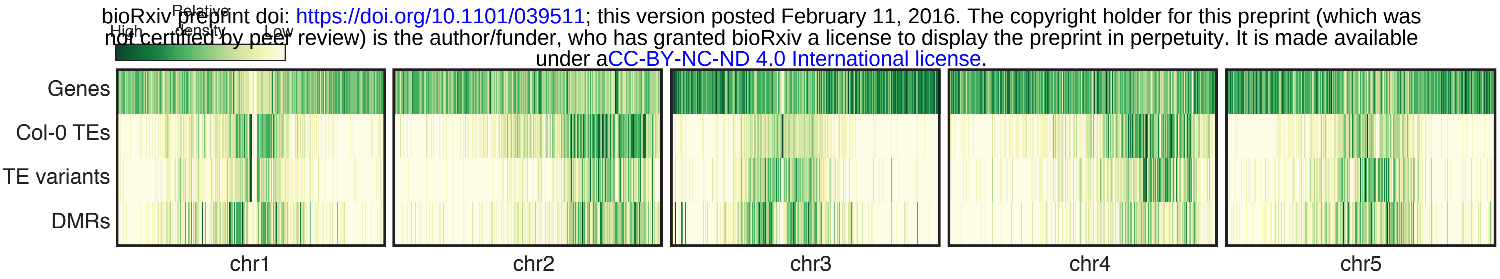
Relative density
High
Low
Genes
Col-0 TEs
TE variants
DMRs
chr1
chr2
chr3
chr4
chr5

Figure S3. Chromosomal distributions of genes, Col-0 TEs, TE variants and population DMRs

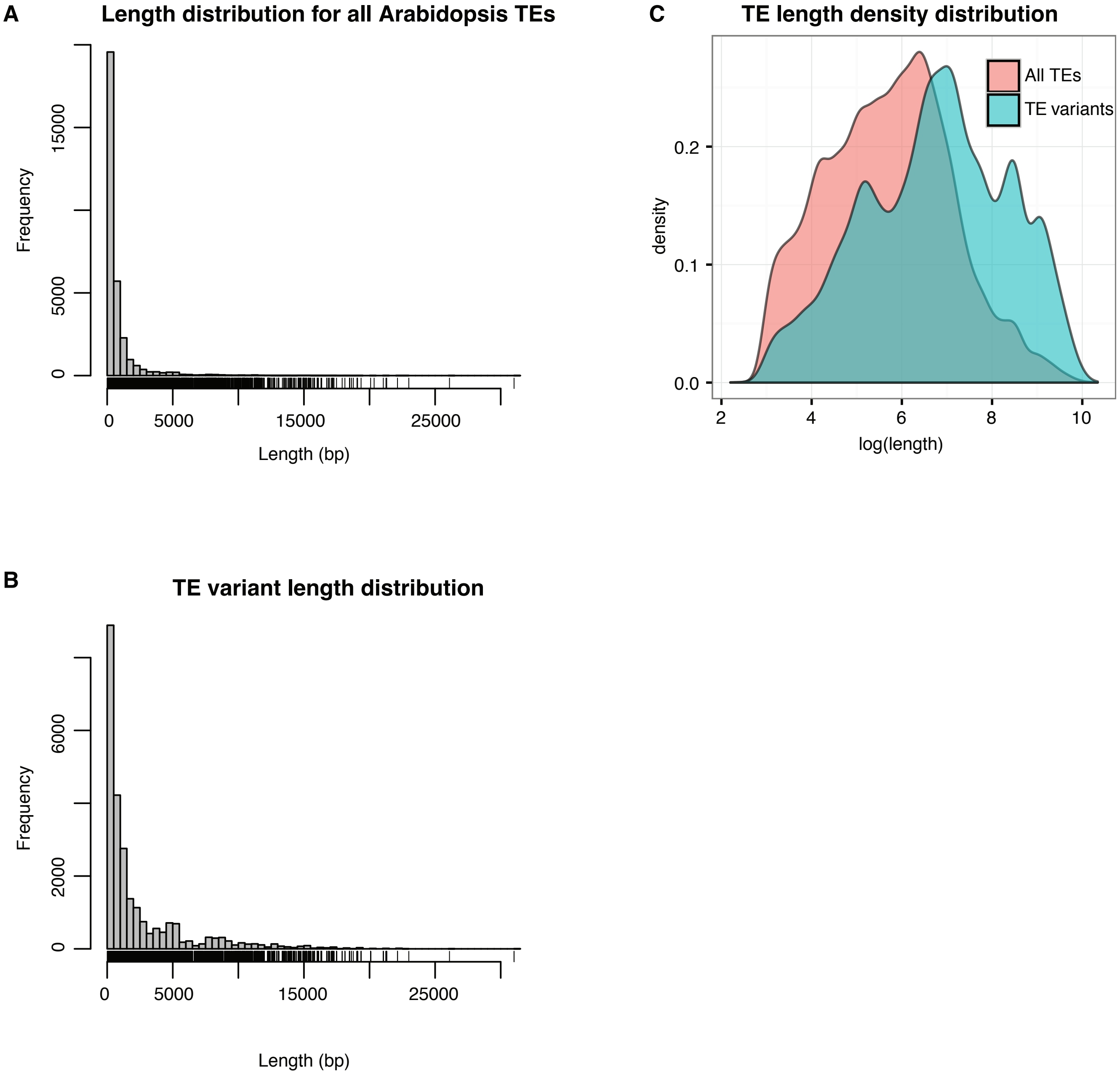
A
Length distribution for all Arabidopsis TEs
Frequency
0
5000
15000
0
5000
15000
25000
Length (bp)
C
TE length density distribution
density
0.0
0.1
0.2
2
4
6
8
10
log(length)
All TEs
TE variants
B
TE variant length distribution
Frequency
0
2000
6000
0
5000
15000
25000
Length (bp)

Figure S4. Length distributions for all Col-0 TEs and TE variants

(A) Histogram showing lengths of all annotated TEs in the Col-0 reference genome.

(B) Histogram showing lengths of all TE variants.

(C) Density distribution of $\log_{10}$ TE length for all Col-0 TEs (red) and TE variants (blue).

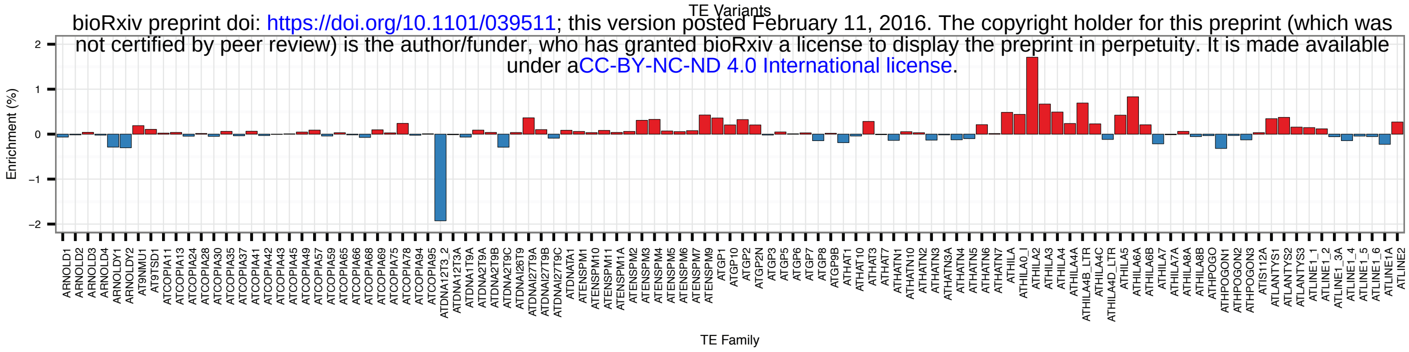
TE Variants
Enrichment (%)
2
1
0
−1
−2
ARNOLD1
ARNOLD2
ARNOLD3
ARNOLD4
ARNOLDY1
ARNOLDY2
AT9NMU1
AT9TSD1
ATCOPIA11
ATCOPIA13
ATCOPIA24
ATCOPIA28
ATCOPIA30
ATCOPIA35
ATCOPIA37
ATCOPIA41
ATCOPIA42
ATCOPIA43
ATCOPIA45
ATCOPIA49
ATCOPIA57
ATCOPIA59
ATCOPIA65
ATCOPIA66
ATCOPIA68
ATCOPIA69
ATCOPIA75
ATCOPIA78
ATCOPIA94
ATCOPIA95
ATDNA12T3_2
ATDNA12T3A
ATDNA1T9A
ATDNA2T9A
ATDNA2T9B
ATDNA2T9C
ATDNAI26T9
ATDNAI27T9A
ATDNAI27T9B
ATDNAI27T9C
ATDNATA1
ATENSPM1
ATENSPM10
ATENSPM11
ATENSPM1A
ATENSPM2
ATENSPM3
ATENSPM4
ATENSPM5
ATENSPM6
ATENSPM7
ATENSPM9
ATGP1
ATGP10
ATGP2
ATGP2N
ATGP3
ATGP5
ATGP6
ATGP7
ATGP8
ATGP9B
ATHAT1
ATHAT10
ATHAT3
ATHAT7
ATHATN1
ATHATN10
ATHATN2
ATHATN3
ATHATN3A
ATHATN4
ATHATN5
ATHATN6
ATHATN7
ATHILA
ATHILA0_I
ATHILA2
ATHILA3
ATHILA4
ATHILA4A
ATHILA4B_LTR
ATHILA4C
ATHILA4D_LTR
ATHILA5
ATHILA6A
ATHILA6B
ATHILA7
ATHILA7A
ATHILA8A
ATHILA8B
ATHPOGO
ATHPOGON1
ATHPOGON2
ATHPOGON3
ATIS112A
ATLANTYS1
ATLANTYS2
ATLANTYS3
ATLINE1_1
ATLINE1_2
ATLINE1_3A
ATLINE1_4
ATLINE1_5
ATLINE1_6
ATLINE1A
ATLINE2
TE Family

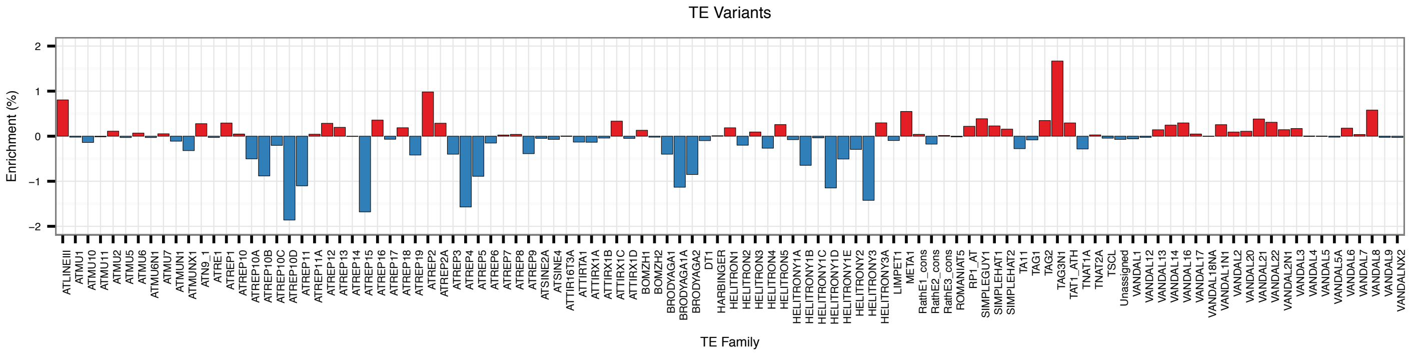
TE Variants
Enrichment (%)
2
1
0
−1
−2
ATLINEIII
ATMU1
ATMU10
ATMU11
ATMU2
ATMU5
ATMU6
ATMU6N1
ATMU7
ATMUN1
ATMUNX1
ATN9_1
ATRE1
ATREP1
ATREP10
ATREP10A
ATREP10B
ATREP10C
ATREP10D
ATREP11
ATREP11A
ATREP12
ATREP13
ATREP14
ATREP15
ATREP16
ATREP17
ATREP18
ATREP19
ATREP2
ATREP2A
ATREP3
ATREP4
ATREP5
ATREP6
ATREP7
ATREP8
ATREP9
ATSINE2A
ATSINE4
ATTIR16T3A
ATTIRTA1
ATTIRX1A
ATTIRX1B
ATTIRX1C
ATTIRX1D
BOMZH1
BOMZH2
BRODYAGA1
BRODYAGA1A
BRODYAGA2
DT1
HARBINGER
HELITRON1
HELITRON2
HELITRON3
HELITRON4
HELITRON5
HELITRONY1A
HELITRONY1B
HELITRONY1C
HELITRONY1D
HELITRONY1E
HELITRONY2
HELITRONY3
HELITRONY3A
LIMPET1
META1
RathE1_cons
RathE2_cons
RathE3_cons
ROMANIAT5
RP1_AT
SIMPLEGUY1
SIMPLEHAT1
SIMPLEHAT2
TA11
TAG1
TAG2
TAG3N1
TAT1_ATH
TNAT1A
TNAT2A
TSCL
Unassigned
VANDAL1
VANDAL12
VANDAL13
VANDAL14
VANDAL16
VANDAL17
VANDAL18NA
VANDAL1N1
VANDAL2
VANDAL20
VANDAL21
VANDAL22
VANDAL2N1
VANDAL3
VANDAL4
VANDAL5
VANDAL5A
VANDAL6
VANDAL7
VANDAL8
VANDAL9
VANDALNX2
TE Family

Figure S5. TE variant enrichment and depletion for all TE families

The percentage of TE variants by TE families were compared to the percentage expected due to the genomic frequency of elements of each TE family. Families with more TE presence/absence variants than expected are plotted in red, indicating percentage enrichment of those elements, while those with a lower number of TE variants than expected are plotted in blue, indicating percentage depletion for that TE family.

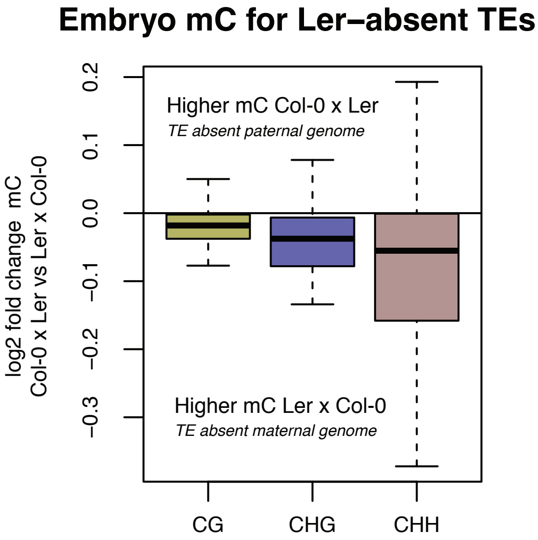
Embryo mC for Ler–absent TEs
log2 fold change mC
Col-0 x Ler vs Ler x Col-0
0.2
0.1
0.0
−0.1
−0.2
−0.3
Higher mC Col-0 x Ler
TE absent paternal genome
Higher mC Ler x Col-0
TE absent maternal genome
CG
CHG
CHH

Figure S6. TE DNA methylation in embryos resulting from a Col-0 x L*er* cross

DNA methylation levels in sperm-demethylated TEs absent from L*er* but present in Col-0. Levels are $\log_2$ fold change mC/C, for each DNA methylation context, between L*er* x Col-0 and Col-0 x L*er* DNA methylation levels. Positive values indicate higher methylation in the L*er* x Col-0 (*female x male*) cross, whereas negative values represent higher methylation in the Col-0 x L*er* cross. Boxplots were constructed as for Fig. 4C.

TABLES

Table 1. Mapping of paired-end reads providing evidence for TE presence/absence variants in L*er* to Col-0 and L*er* reference genomes.

	Concordant	**Discordant**	**Split**	**Unmapped**	**Total**
Col-0 mapped	0	993	9,513	0	10,206
Ler mapped	10,073	92	34	7	10,206

Table 2. Significantly differentially expressed genes dependent on TE presence/absence.

TE insertion point	AGI	Gene name	Function	Pearson correlation	log2 fold change FPKM	p-value	q-value
Exon	AT1G28620	-	Lipase	0.27	-3.71	2.74E-06	1.73E-04
	AT1G31580	*ECS1*	Cell wall protein related to Xanthomonas campestris pv. campestris resistance	0.28	-2.91	9.43E-10	2.49E-07
	AT1G48820	-	Terpenoid cyclase	0.27	-2.66	1.86E-05	7.46E-04
	AT2G15040	*AtRLP18*	Disease resistance protein	0.49	-1.62	5.80E-10	2.42E-07
	AT2G16520	-	-	-0.53	3.07	1.76E-10	9.05E-08
	AT2G16810	-	F-box protein	-0.48	2.36	1.86E-05	7.46E-04
	AT3G19520	-	-	0.68	-2.61	9.98E-08	1.14E-05
	AT3G26230	*CYP71B24*	Cytochrome P450	0.53	-2.40	6.44E-13	6.63E-10
	AT3G46482	-	-	-0.48	4.46	2.05E-09	4.52E-07
	AT3G62460	-	Putative endonuclease	0.20	-2.56	9.03E-08	1.12E-05
	AT4G05500	-	F-box protein	-0.44	1.26	5.13E-06	2.66E-04
	AT4G15056	-	-	-0.60	4.63	4.25E-06	2.34E-04
	AT5G16990	-	Oxidative stress tolerance	-0.49	1.02	5.26E-06	2.66E-04
	AT5G38565	-	F-box protein	0.35	-1.84	2.13E-06	1.44E-04
	AT5G67310	*CYP81G1*	Cytochrome P450	0.22	-3.53	3.61E-07	3.47E-05
Intron	AT1G48820	-	Terpenoid cyclase	0.27	-2.66	1.86E-05	7.46E-04
	AT1G52710	-	Cytochrome-c oxidase activity	0.30	-2.57	8.30E-06	4.07E-04
	AT2G03913	-	Defensin-like family protein	-0.72	8.35	1.64E-17	5.06E-14
	AT3G59190	-	F-box protein	0.29	-3.39	4.13E-09	8.50E-07
	AT3G62460	-	Putative endonuclease	0.20	-2.56	9.03E-08	1.12E-05
	AT4G15056	-	-	-0.60	4.63	4.25E-06	2.34E-04
3' UTR	AT5G38565	-	F-box protein	0.35	-1.84	2.13E-06	1.44E-04
5' UTR	AT1G31580	*ECS1*	Cell wall protein related to Xanthomonas campestris pv. campestris resistance	0.28	-2.91	9.43E-10	2.49E-07
	AT2G16810	-	F-box protein	-0.48	2.36	1.86E-05	7.46E-04
	AT5G16990	-	Oxidative stress tolerance	-0.49	1.02	5.26E-06	2.66E-04
Upstream	AT1G48700	-	Oxidoreductase activity	-0.42	1.56	4.31E-07	3.91E-05
	AT1G61415	-	-	-0.38	1.90	8.52E-07	6.74E-05
	AT2G01360	-	PPR protein	-0.84	5.06	1.80E-07	1.80E-05
	AT2G16520	-	-	-0.53	3.07	1.76E-10	9.05E-08
	AT2G16530	*PPRD2*	Oxidoreductase activity	0.42	-1.01	1.05E-07	1.16E-05
	AT2G17080	-	-	-0.49	2.65	1.15E-08	1.97E-06
	AT2G25510	-	-	0.43	-2.49	2.52E-08	3.89E-06

	AT4G11290	*AtPrx39*	Peroxidase activity, cold tolerance	0.35	-1.43	2.15E-06	1.44E-04
	AT4G15620	*CASPL1E2*	-	0.38	-1.70	3.29E-08	4.61E-06
	AT5G28010	-	Defence response	0.38	-1.76	9.69E-10	2.49E-07
	AT5G32620	-	-	-0.36	2.27	3.03E-08	4.45E-06
	AT5G38565	-	F-box protein	0.35	-1.84	2.13E-06	1.44E-04
	AT5G49500	-	Signal recognition particle	-0.41	1.62	2.29E-05	8.93E-04
	AT5G66660	-	-	-0.39	1.03	1.55E-05	7.03E-04
Downstream	AT1G02770	-	-	-0.46	1.36	3.71E-07	3.47E-05
	AT1G33930	-	GTP binding	0.55	-2.61	3.57E-15	5.51E-12
	AT1G77960	-	-	0.15	-4.51	4.22E-06	2.34E-04
	AT2G12460	-	-	0.29	-2.65	7.07E-07	5.74E-05
	AT2G16810	-	F-box protein	-0.48	2.36	1.86E-05	7.46E-04
	AT2G19400	-	Kinase	0.42	-1.54	1.40E-06	1.08E-04
	AT2G27650	-	Ubiquitin thiolesterase activity	-0.41	1.20	7.88E-06	3.93E-04
	AT3G46482	-	-	-0.48	4.46	2.05E-09	4.52E-07
	AT4G03050	*AOP3*	Glucosinolate biosynthesis	-0.38	2.39	4.82E-07	4.13E-05
	AT4G07820	-	-	0.29	-2.78	1.48E-06	1.11E-04
	AT5G16990	-	Oxidative stress tolerance	-0.49	1.02	5.26E-06	2.66E-04
	AT5G22608	-	-	0.33	-1.94	4.76E-07	4.13E-05
	AT5G23770	*AtDUF8*	-	-0.56	1.53	5.50E-07	4.59E-05
	AT5G24570	-	-	0.27	-1.01	2.43E-05	9.37E-04
	AT5G27340	-	-	-0.41	4.08	4.26E-08	5.72E-06
	AT5G35796	-	-	-0.50	1.36	7.65E-09	1.39E-06
	AT5G45840	-	Protein kinase activity	0.25	-3.22	1.51E-06	1.11E-04
	AT5G66455	-	PPR pseudogene	0.32	-1.44	1.39E-05	6.52E-04

1001 **Table S1. TE superfamily enrichments for TE variants**

TE superfamily	Genomic count	Variant count	Genomic frequency	Variant frequency	Enrichment (%)
DNA	1829	798	5.86E+00	3.76E-02	-2.10
DNA/En-Spm	941	933	3.02E+00	4.40E-02	1.38
DNA/Harbinger	379	339	1.22E+00	1.60E-02	0.38
DNA/HAT	1035	1109	3.32E+00	5.23E-02	1.91
DNA/Mariner	151	98	4.84E-01	4.62E-03	-0.02
DNA/MuDR	5410	3777	1.73E+01	1.78E-01	0.45
DNA/Pogo	344	127	1.10E+00	5.98E-03	-0.50
DNA/Tc1	95	37	3.05E-01	1.74E-03	-0.13
LINE	81	45	2.60E-01	2.12E-03	-0.05
LINE/L1	1366	1017	4.38E+00	4.79E-02	0.41
LTR/Copia	1781	1747	5.71E+00	8.23E-02	2.52
LTR/Gypsy	4181	4442	1.34E+01	2.09E-01	7.53
RathE1_cons	213	150	6.83E-01	7.07E-03	0.02
RathE2_cons	74	14	2.37E-01	6.60E-04	-0.17
RathE3_cons	104	72	3.33E-01	3.39E-03	0.01
RC/Helitron	12945	6372	4.15E+01	3.00E-01	-11.48
SINE	131	64	4.20E-01	3.02E-03	-0.12
Unassigned	129	80	4.14E-01	3.77E-03	-0.04

1002

1003 **Table S2. TE family enrichments for TE variants.**

TE family	Genomic count	Variant count	Genomic frequency	Variant frequency	Enrichment (%)
ARNOLD1	39	13	1.30E-01	6.48E-04	-0.06
ARNOLD2	68	42	2.26E-01	2.09E-03	-0.02
ARNOLD3	45	38	1.49E-01	1.90E-03	0.04
ARNOLD4	23	11	7.64E-02	5.49E-04	-0.02
ARNOLDY1	237	100	7.87E-01	4.99E-03	-0.29
ARNOLDY2	288	131	9.56E-01	6.53E-03	-0.30
AT9NMU1	45	68	1.49E-01	3.39E-03	0.19
AT9TSD1	55	58	1.83E-01	2.89E-03	0.11
ATCOPIA11	26	22	8.63E-02	1.10E-03	0.02
ATCOPIA13	35	31	1.16E-01	1.55E-03	0.04
ATCOPIA24	27	9	8.97E-02	4.49E-04	-0.04
ATCOPIA28	81	57	2.69E-01	2.84E-03	0.02
ATCOPIA30	33	12	1.10E-01	5.99E-04	-0.05
ATCOPIA35	22	27	7.31E-02	1.35E-03	0.06
ATCOPIA37	32	14	1.06E-01	6.98E-04	-0.04
ATCOPIA41	39	39	1.30E-01	1.95E-03	0.07
ATCOPIA42	35	17	1.16E-01	8.48E-04	-0.03
ATCOPIA43	29	18	9.63E-02	8.98E-04	-0.01
ATCOPIA45	20	14	6.64E-02	6.98E-04	0.00
ATCOPIA49	34	32	1.13E-01	1.60E-03	0.05
ATCOPIA57	48	50	1.59E-01	2.49E-03	0.09
ATCOPIA59	20	5	6.64E-02	2.49E-04	-0.04
ATCOPIA65	34	29	1.13E-01	1.45E-03	0.03
ATCOPIA66	20	10	6.64E-02	4.99E-04	-0.02
ATCOPIA68	43	14	1.43E-01	6.98E-04	-0.07
ATCOPIA69	25	36	8.30E-02	1.80E-03	0.10
ATCOPIA75	20	19	6.64E-02	9.48E-04	0.03
ATCOPIA78	24	64	7.97E-02	3.19E-03	0.24
ATCOPIA94	39	21	1.30E-01	1.05E-03	-0.02
ATCOPIA95	72	49	2.39E-01	2.44E-03	0.01
ATDNA12T3_2	660	53	2.19E+00	2.64E-03	-1.93
ATDNA12T3A	22	12	7.31E-02	5.99E-04	-0.01
ATDNA1T9A	36	11	1.20E-01	5.49E-04	-0.06
ATDNA2T9A	48	50	1.59E-01	2.49E-03	0.09
ATDNA2T9B	26	25	8.63E-02	1.25E-03	0.04
ATDNA2T9C	242	103	8.04E-01	5.14E-03	-0.29
ATDNAI26T9	25	24	8.30E-02	1.20E-03	0.04
ATDNAI27T9A	116	150	3.85E-01	7.48E-03	0.36
ATDNAI27T9B	43	49	1.43E-01	2.44E-03	0.10
ATDNAI27T9C	108	54	3.59E-01	2.69E-03	-0.09
ATDNATA1	28	36	9.30E-02	1.80E-03	0.09
ATENSPM1	30	32	9.96E-02	1.60E-03	0.06

ATENSPM10	81	61	2.69E-01	3.04E-03	0.04
ATENSPM11	47	48	1.56E-01	2.39E-03	0.08
ATENSPM1A	77	59	2.56E-01	2.94E-03	0.04
ATENSPM2	114	88	3.79E-01	4.39E-03	0.06
ATENSPM3	98	127	3.25E-01	6.33E-03	0.31
ATENSPM4	50	99	1.66E-01	4.94E-03	0.33
ATENSPM5	111	88	3.69E-01	4.39E-03	0.07
ATENSPM6	151	112	5.01E-01	5.59E-03	0.06
ATENSPM7	74	65	2.46E-01	3.24E-03	0.08
ATENSPM9	97	150	3.22E-01	7.48E-03	0.43
ATGP1	144	168	4.78E-01	8.38E-03	0.36
ATGP10	165	151	5.48E-01	7.53E-03	0.21
ATGP2	48	97	1.59E-01	4.84E-03	0.32
ATGP2N	54	77	1.79E-01	3.84E-03	0.20
ATGP3	60	36	1.99E-01	1.80E-03	-0.02
ATGP5	86	67	2.86E-01	3.34E-03	0.05
ATGP6	25	18	8.30E-02	8.98E-04	0.01
ATGP7	47	37	1.56E-01	1.85E-03	0.03
ATGP8	92	32	3.06E-01	1.60E-03	-0.15
ATGP9B	27	22	8.97E-02	1.10E-03	0.02
ATHAT1	105	32	3.49E-01	1.60E-03	-0.19
ATHAT10	35	15	1.16E-01	7.48E-04	-0.04
ATHAT3	23	72	7.64E-02	3.59E-03	0.28
ATHAT7	20	11	6.64E-02	5.49E-04	-0.01
ATHATN1	69	18	2.29E-01	8.98E-04	-0.14
ATHATN10	48	43	1.59E-01	2.14E-03	0.06
ATHATN2	46	37	1.53E-01	1.85E-03	0.03
ATHATN3	70	20	2.32E-01	9.98E-04	-0.13
ATHATN3A	20	10	6.64E-02	4.99E-04	-0.02
ATHATN4	56	12	1.86E-01	5.99E-04	-0.13
ATHATN5	42	8	1.39E-01	3.99E-04	-0.10
ATHATN6	43	71	1.43E-01	3.54E-03	0.21
ATHATN7	71	50	2.36E-01	2.49E-03	0.01
ATHILA	198	229	6.58E-01	1.14E-02	0.48
ATHILA0_I	138	180	4.58E-01	8.98E-03	0.44
ATHILA2	413	618	1.37E+00	3.08E-02	1.71
ATHILA3	243	296	8.07E-01	1.48E-02	0.67
ATHILA4	250	265	8.30E-01	1.32E-02	0.49
ATHILA4A	310	254	1.03E+00	1.27E-02	0.24
ATHILA4B_LTR	143	234	4.75E-01	1.17E-02	0.69
ATHILA4C	206	183	6.84E-01	9.13E-03	0.23
ATHILA4D_LTR	106	47	3.52E-01	2.34E-03	-0.12
ATHILA5	131	172	4.35E-01	8.58E-03	0.42
ATHILA6A	247	331	8.20E-01	1.65E-02	0.83
ATHILA6B	134	131	4.45E-01	6.53E-03	0.21

ATHILA7	134	46	4.45E-01	2.29E-03	-0.22
ATHILA7A	31	18	1.03E-01	8.98E-04	-0.01
ATHILA8A	97	77	3.22E-01	3.84E-03	0.06
ATHILA8B	78	41	2.59E-01	2.04E-03	-0.05
ATHPOGO	25	10	8.30E-02	4.99E-04	-0.03
ATHPOGON1	174	52	5.78E-01	2.59E-03	-0.32
ATHPOGON2	27	12	8.97E-02	5.99E-04	-0.03
ATHPOGON3	118	53	3.92E-01	2.64E-03	-0.13
ATIS112A	173	122	5.75E-01	6.09E-03	0.03
ATLANTYS1	153	171	5.08E-01	8.53E-03	0.34
ATLANTYS2	179	194	5.94E-01	9.68E-03	0.37
ATLANTYS3	142	126	4.72E-01	6.28E-03	0.16
ATLINE1_1	61	70	2.03E-01	3.49E-03	0.15
ATLINE1_2	41	51	1.36E-01	2.54E-03	0.12
ATLINE1_3A	160	95	5.31E-01	4.74E-03	-0.06
ATLINE1_4	102	39	3.39E-01	1.95E-03	-0.14
ATLINE1_5	91	52	3.02E-01	2.59E-03	-0.04
ATLINE1_6	129	75	4.28E-01	3.74E-03	-0.05
ATLINE1A	289	147	9.60E-01	7.33E-03	-0.23
ATLINE2	138	146	4.58E-01	7.28E-03	0.27
ATLINEIII	196	292	6.51E-01	1.46E-02	0.81
ATMU1	59	35	1.96E-01	1.75E-03	-0.02
ATMU10	87	30	2.89E-01	1.50E-03	-0.14
ATMU11	20	11	6.64E-02	5.49E-04	-0.01
ATMU2	64	65	2.13E-01	3.24E-03	0.11
ATMU5	24	10	7.97E-02	4.99E-04	-0.03
ATMU6	26	31	8.63E-02	1.55E-03	0.07
ATMU6N1	39	20	1.30E-01	9.98E-04	-0.03
ATMU7	32	32	1.06E-01	1.60E-03	0.05
ATMUN1	107	49	3.55E-01	2.44E-03	-0.11
ATMUNX1	155	39	5.15E-01	1.95E-03	-0.32
ATN9_1	65	99	2.16E-01	4.94E-03	0.28
ATRE1	22	9	7.31E-02	4.49E-04	-0.03
ATREP1	498	390	1.65E+00	1.95E-02	0.29
ATREP10	63	51	2.09E-01	2.54E-03	0.05
ATREP10A	279	85	9.27E-01	4.24E-03	-0.50
ATREP10B	491	150	1.63E+00	7.48E-03	-0.88
ATREP10C	123	41	4.08E-01	2.04E-03	-0.20
ATREP10D	1295	489	4.30E+00	2.44E-02	-1.86
ATREP11	841	339	2.79E+00	1.69E-02	-1.10
ATREP11A	95	72	3.15E-01	3.59E-03	0.04
ATREP12	22	72	7.31E-02	3.59E-03	0.29
ATREP13	106	110	3.52E-01	5.49E-03	0.20
ATREP14	47	30	1.56E-01	1.50E-03	-0.01
ATREP15	1003	331	3.33E+00	1.65E-02	-1.68

ATREP16	47	103	1.56E-01	5.14E-03	0.36
ATREP17	34	9	1.13E-01	4.49E-04	-0.07
ATREP18	391	298	1.30E+00	1.49E-02	0.19
ATREP19	189	42	6.28E-01	2.09E-03	-0.42
ATREP2	164	306	5.45E-01	1.53E-02	0.98
ATREP2A	116	135	3.85E-01	6.73E-03	0.29
ATREP3	1439	878	4.78E+00	4.38E-02	-0.40
ATREP4	832	239	2.76E+00	1.19E-02	-1.57
ATREP5	624	237	2.07E+00	1.18E-02	-0.89
ATREP6	181	90	6.01E-01	4.49E-03	-0.15
ATREP7	164	114	5.45E-01	5.69E-03	0.02
ATREP8	75	58	2.49E-01	2.89E-03	0.04
ATREP9	201	56	6.67E-01	2.79E-03	-0.39
ATSINE2A	33	13	1.10E-01	6.48E-04	-0.04
ATSINE4	98	51	3.25E-01	2.54E-03	-0.07
ATTIR16T3A	106	71	3.52E-01	3.54E-03	0.00
ATTIRTA1	95	37	3.15E-01	1.85E-03	-0.13
ATTIRX1A	63	15	2.09E-01	7.48E-04	-0.13
ATTIRX1B	44	21	1.46E-01	1.05E-03	-0.04
ATTIRX1C	39	93	1.30E-01	4.64E-03	0.33
ATTIRX1D	28	9	9.30E-02	4.49E-04	-0.05
BOMZH1	28	45	9.30E-02	2.24E-03	0.13
BOMZH2	47	27	1.56E-01	1.35E-03	-0.02
BRODYAGA1	251	87	8.34E-01	4.34E-03	-0.40
BRODYAGA1A	586	163	1.95E+00	8.13E-03	-1.13
BRODYAGA2	525	179	1.74E+00	8.93E-03	-0.85
DT1	123	62	4.08E-01	3.09E-03	-0.10
HARBINGER	90	62	2.99E-01	3.09E-03	0.01
HELITRON1	130	124	4.32E-01	6.18E-03	0.19
HELITRON2	194	89	6.44E-01	4.44E-03	-0.20
HELITRON3	53	54	1.76E-01	2.69E-03	0.09
HELITRON4	199	79	6.61E-01	3.94E-03	-0.27
HELITRON5	56	89	1.86E-01	4.44E-03	0.26
HELITRONY1A	271	165	9.00E-01	8.23E-03	-0.08
HELITRONY1B	414	146	1.37E+00	7.28E-03	-0.65
HELITRONY1C	120	73	3.98E-01	3.64E-03	-0.03
HELITRONY1D	756	273	2.51E+00	1.36E-02	-1.15
HELITRONY1E	447	196	1.48E+00	9.78E-03	-0.51
HELITRONY2	198	73	6.58E-01	3.64E-03	-0.29
HELITRONY3	1399	646	4.65E+00	3.22E-02	-1.42
HELITRONY3A	49	92	1.63E-01	4.59E-03	0.30
LIMPET1	116	58	3.85E-01	2.89E-03	-0.10
META1	138	202	4.58E-01	1.01E-02	0.55
RathE1_cons	213	150	7.07E-01	7.48E-03	0.04
RathE2_cons	74	14	2.46E-01	6.98E-04	-0.18

RathE3_cons	104	72	3.45E-01	3.59E-03	0.01
ROMANIAT5	49	30	1.63E-01	1.50E-03	-0.01
RP1_AT	87	102	2.89E-01	5.09E-03	0.22
SIMPLEGUY1	116	155	3.85E-01	7.73E-03	0.39
SIMPLEHAT1	56	83	1.86E-01	4.14E-03	0.23
SIMPLEHAT2	73	80	2.42E-01	3.99E-03	0.16
TA11	157	49	5.21E-01	2.44E-03	-0.28
TAG1	28	2	9.30E-02	9.98E-05	-0.08
TAG2	86	127	2.86E-01	6.33E-03	0.35
TAG3N1	97	399	3.22E-01	1.99E-02	1.67
TAT1_ATH	87	117	2.89E-01	5.84E-03	0.29
TNAT1A	162	51	5.38E-01	2.54E-03	-0.28
TNAT2A	38	31	1.26E-01	1.55E-03	0.03
TSCL	81	45	2.69E-01	2.24E-03	-0.04
Unassigned	113	61	3.75E-01	3.04E-03	-0.07
VANDAL1	80	42	2.66E-01	2.09E-03	-0.06
VANDAL12	37	20	1.23E-01	9.98E-04	-0.02
VANDAL13	38	54	1.26E-01	2.69E-03	0.14
VANDAL14	25	66	8.30E-02	3.29E-03	0.25
VANDAL16	42	87	1.39E-01	4.34E-03	0.29
VANDAL17	178	128	5.91E-01	6.38E-03	0.05
VANDAL18NA	24	15	7.97E-02	7.48E-04	0.00
VANDAL1N1	52	86	1.73E-01	4.29E-03	0.26
VANDAL2	43	47	1.43E-01	2.34E-03	0.09
VANDAL20	51	56	1.69E-01	2.79E-03	0.11
VANDAL21	64	119	2.13E-01	5.94E-03	0.38
VANDAL22	48	94	1.59E-01	4.69E-03	0.31
VANDAL2N1	51	63	1.69E-01	3.14E-03	0.14
VANDAL3	177	152	5.88E-01	7.58E-03	0.17
VANDAL4	102	68	3.39E-01	3.39E-03	0.00
VANDAL5	85	56	2.82E-01	2.79E-03	0.00
VANDAL5A	56	33	1.86E-01	1.65E-03	-0.02
VANDAL6	89	95	2.96E-01	4.74E-03	0.18
VANDAL7	36	31	1.20E-01	1.55E-03	0.04
VANDAL8	123	198	4.08E-01	9.88E-03	0.58
VANDAL9	43	24	1.43E-01	1.20E-03	-0.02
VANDALNX2	37	19	1.23E-01	9.48E-04	-0.03